Altered glycosylation of IgG4 promotes lectin complement pathway activation in anti-PL A2R1-associated membranous nephropathy

Haddad, G.; Lorenzen, J.M.; Ma, H.; Haan, N. de; Seeger, H.; Zaghrini, C.; ... ; Kistler, A.D.

Citation

Note: To cite this publication please use the final published version (if applicable).

Altered glycosylation of IgG4 promotes lectin complement pathway activation in anti-PLA2R1–associated membranous nephropathy

George Haddad,[1,2] Johan M. Lorenzen,[1,2] Hong Ma,[3] Noortje de Haan,[4] Harald Seeger,[1,2] Christelle Zaghrini,[5] Simone Brandt,[6] Malte Kölling,[1] Urs Wegmann,[1] Bence Kiss,[7] Gábor Pál,[7] Péter Gál,[8] Rudolf P. Wüthrich,[1,2] Manfred Wuhrer,[4] Laurence H. Beck,[3] David J. Salant,[3] Gérard Lambeau,[5] and Andreas D. Kistler[1,2,9]

[1]Institute of Physiology, University of Zurich, Switzerland. [2]Division of Nephrology, University Hospital of Zurich, Switzerland. [3]Department of Medicine, Boston University School of Medicine, Boston, Massachusetts, USA. [4]Center for Proteomics and Metabolomics, Leiden University Medical Center, Netherlands. [5]Université Côte d'Azur, CNRS, Institut de Pharmacologie Moléculaire et Cellulaire, Valbonne Sophia Antipolis, France. [6]Institute of Pathology, University Hospital of Zurich, Switzerland. [7]Department of Biochemistry, Eötvös Loránd University, Budapest, Hungary. [8]Institute of Enzymology, Research Centre for Natural Sciences, Budapest, Hungary. [9]Department of Medicine, Cantonal Hospital Frauenfeld, Switzerland.

Primary membranous nephropathy (pMN) is a leading cause of nephrotic syndrome in adults. In most cases, this autoimmune kidney disease is associated with autoantibodies against the M-type phospholipase A2 receptor (PLA2R1) expressed on kidney podocytes, but the mechanisms leading to glomerular damage remain elusive. Here, we developed a cell culture model using human podocytes and found that anti-PLA2R1–positive pMN patient sera or isolated IgG4, but not IgG4-depleted sera, induced proteolysis of the 2 essential podocyte proteins synaptopodin and NEPH1 in the presence of complement, resulting in perturbations of the podocyte cytoskeleton. Specific blockade of the lectin pathway prevented degradation of synaptopodin and NEPH1. Anti-PLA2R1 IgG4 directly bound mannose-binding lectin in a glycosylation-dependent manner. In a cohort of pMN patients, we identified increased levels of galactose-deficient IgG4, which correlated with anti-PLA2R1 titers and podocyte damage induced by patient sera. Assembly of the terminal C5b-9 complement complex and activation of the complement receptors C3aR1 or C5aR1 were required to induce proteolysis of synaptopodin and NEPH1 by 2 distinct proteolytic pathways mediated by cysteine and aspartic proteinases, respectively. Together, these results demonstrated a mechanism by which aberrantly glycosylated IgG4 activated the lectin pathway and induced podocyte injury in primary membranous nephropathy.

Introduction

Primary membranous nephropathy (pMN) is an organ-specific autoimmune kidney disease caused by circulating autoantibodies that target surface antigens on glomerular podocytes (1–3). The M-type phospholipase A2 receptor (PLA2R1) is the predominant autoantigen in adults with pMN, and circulating anti-PLA2R1 antibodies are found in 70%–80% of cases (4). The antigen and bound antibodies are shed from the cell surface to form subepithelial immune complexes associated with glomerular basement membrane (GBM) remodeling and profound changes in the structure and function of the podocytes, such that the normal permeability barrier is breached and plasma proteins leak into the urine (proteinuria), causing body swelling (nephrotic syndrome, refs. 1–3, 5). Remarkably, the immune deposits in pMN contain substantial amounts of complement, including C3 and C5 cleavage products and the terminal C5b-9 complex, yet the predominant IgG subclass in pMN is IgG4, which is incapable of activating complement via the classical pathway (6). Thus, it is unclear how complement is activated in pMN and whether or not it is actually responsible for podocyte injury.

Evidence that complement is important for the development of podocyte injury and proteinuria in pMN is derived mostly from the Heymann nephritis model of membranous nephropathy in rats induced by antibodies against megalin (5). However, there is no suitable experimental model to test the ability of human anti-PLA2R1 autoantibodies to activate complement in vivo because rodents do not express PLA2R1 on their podocytes. Even a recently reported mouse model based on transgenic expression of PLA2R1 in podocytes (7) did not recapitulate the human disease because of the differences between rodent and human IgG subclasses and their capabilities to bind complement. Immunohistology provides clues about which of the 3 types of complement pathways might be activated in pMN. C1q is generally absent from the C3-containing

immune deposits in pMN (8–11), which suggests the possibility that the alternative or lectin pathways may be involved, instead of the classical pathway. Of the two, the lectin pathway, acting through mannose binding lectin–associated (MBL-associated) serine proteases (MASPs) 1 and 2 seems a better candidate (12, 13), because C4d, a product of MASP-induced C4 cleavage, is commonly found in pMN (14), whereas the alternative pathway does not cleave C4. In addition, MBL has been identified in the glomeruli in a substantial proportion of cases of pMN, where it colocalizes with PLA2R1 (8, 15, 16). Although there is no evidence that IgG4 can activate the lectin pathway, it has been shown that IgG autoantibodies lacking the terminal galactose residues at position Asn 297 of the constant fragment (Fc) (agalactosyl oligosaccharide, G0) are able to bind and activate MBL (17).

If indeed complement activation is responsible for podocyte injury in pMN, the mechanisms and consequences of such injury will need to be established. Permselectivity of the glomerular filtration barrier is ensured through interdigitating cellular processes, called podocyte foot processes, that are maintained by a complex cytoskeletal network and connected through a membrane-like structure, the slit diaphragm. Proteinuric kidney diseases, including membranous nephropathy, are characterized by the loss of these foot processes (foot process effacement) through perturbations of slit diaphragm proteins, such as nephrin, podocin, and NEPH1, and proteins that regulate cytoskeletal structure and dynamics, including synaptopodin, alpha-actinin 4, dynamin, and Rho-GTPases (18). Alterations in the podocyte actin cytoskeleton and slit diaphragm–associated proteins have been documented in human and experimental membranous nephropathy (19, 20). Moreover, a variety of signaling events have been identified in in vitro models of antibody- and complement-mediated podocyte injury (5, 21, 22), but the mechanisms linking these pathways to slit diaphragm and cytoskeletal proteins remain elusive. Furthermore, these in vitro models were based on rodent podocytes and nonhuman antibodies against antigens other than PLA2R1. Nevertheless, they suggest an avenue to determine whether similar mechanisms may be operative when anti-PLA2R1 activates complement on the cell surface of human podocytes.

Here, we have established an in vitro model based on human podocytes expressing PLA2R1 and patient sera or IgG4. We showed that anti-PLA2R1 IgG4 autoantibodies were able to activate the lectin complement pathway and induce sublethal injury of PLA2R1-expressing podocytes in a glycosylation-dependent manner, and we have identified the cellular pathways mediating such injury. Moreover, patients with pMN exhibited alterations in their IgG4 glycosylation pattern that correlated with disease severity.

Results

Anti-PLA2R1–positive sera induce rapid loss of synaptopodin and NEPH1 in human podocytes. In vivo, PLA2R1 is endogenously expressed at the surface of podocytes present in human glomeruli (4). However, we did not detect relevant levels of PLA2R1 protein in 4 conditionally immortalized human podocyte cell lines, all of which expressed the podocyte markers synaptopodin and NEPH-1 (Supplemental Figure 1; supplemental material available online with this article; https://doi.org/10.1172/JCI140453DS1). We thus used lentiviral gene transfer to express PLA2R1 in differen-

tiated cultured podocytes, resulting in expression levels comparable to those in normal human glomeruli in vivo (Supplemental Figure 2, A–C). The LY-podocyte cell line used for all subsequent experiments expressed the key podocyte proteins synaptopodin, NEPH1, podocalyxin, and podocin when cultured under conditions that induced differentiation of the cells (Supplemental Figure 1E). Lentiviral expression of PLA2R1 did not induce morphological alterations of the cells nor alter synaptopodin and NEPH1 expression levels or their subcellular distribution (Supplemental Figure 2D). In cultured rodent podocytes, addition of anti-podocyte antibodies and cryopreserved serum as a source of complement has previously been shown to induce cell lysis at high concentrations, whereas lower antibody and complement concentrations induce sublytic podocyte injury (22–24). In contrast, treatment of human podocytes expressing PLA2R1 with anti-PLA2R1–positive patient sera and high concentrations of cryopreserved normal human serum (NHS) as a source of functional complement system did not induce cell lysis despite PLA2R1-dependent deposition of complement components (Supplemental Figure 3). Notwithstanding the absence of a lytic effect, we tested for potential sublytic podocyte injury after adding patient sera and NHS in concentrations similar to those applied in experiments with rodent podocytes (22–25). We analyzed the levels of 4 essential podocyte proteins (2 slit diaphragm–associated, 1 actin-associated, and 1 cell surface protein) that have been implicated in podocyte damage as well as 2 of the pathways previously associated with sublytic complement damage in rodent cells, the ERK and the Akt pathways. Whereas podocin and podocalyxin protein levels remained unchanged, we observed a rapid reduction of synaptopodin and NEPH1 levels by Western blot analysis (Figure 1A). Immunofluorescence revealed a reduction and redistribution of synaptopodin and NEPH1 along with a reduction of actin stress fibers and variable degrees of cell rounding (Figure 1B and Supplemental Figure 4). Loss of synaptopodin and NEPH1 was dependent on the expression of PLA2R1, occurred only with high-titer anti-PLA2R1–positive membranous nephropathy sera, required an active complement system, and was independent of the cell line used (Supplemental Figures 5–7). Interestingly, sheep antisera raised against mouse podocyte lysates did not affect synaptopodin and NEPH1 in cultured mouse podocytes, whereas human anti-PLA2R1–positive membranous nephropathy serum had a strong effect on synaptopodin and NEPH1 levels in mouse podocytes expressing PLA2R1 (Supplemental Figure 8). Given the absent effect on podocin protein levels, we also analyzed the transcription of podocin and nephrin, both of which were unaffected (Supplemental Figure 9). ERK and Akt phosphorylation were induced by serum after starvation, but this effect did not depend on PLA2R1 positivity of patient serum, PLA2R1 expression, or an active complement system, and rather tended to be reduced in PLA2R1-expressing cells treated with high-titer serum and complement (Supplemental Figure 6).

We next validated the effect on synaptopodin and NEPH1 in a large cohort of pMN and control patients and observed that it was specific to PLA2R1-associated pMN (Figure 1C) and correlated with the antibody levels as determined by ELISA (Figure 1D). We also detected degradation of synaptopodin and NEPH1 with serum from a patient with treatment-resistant focal segmental glomer-
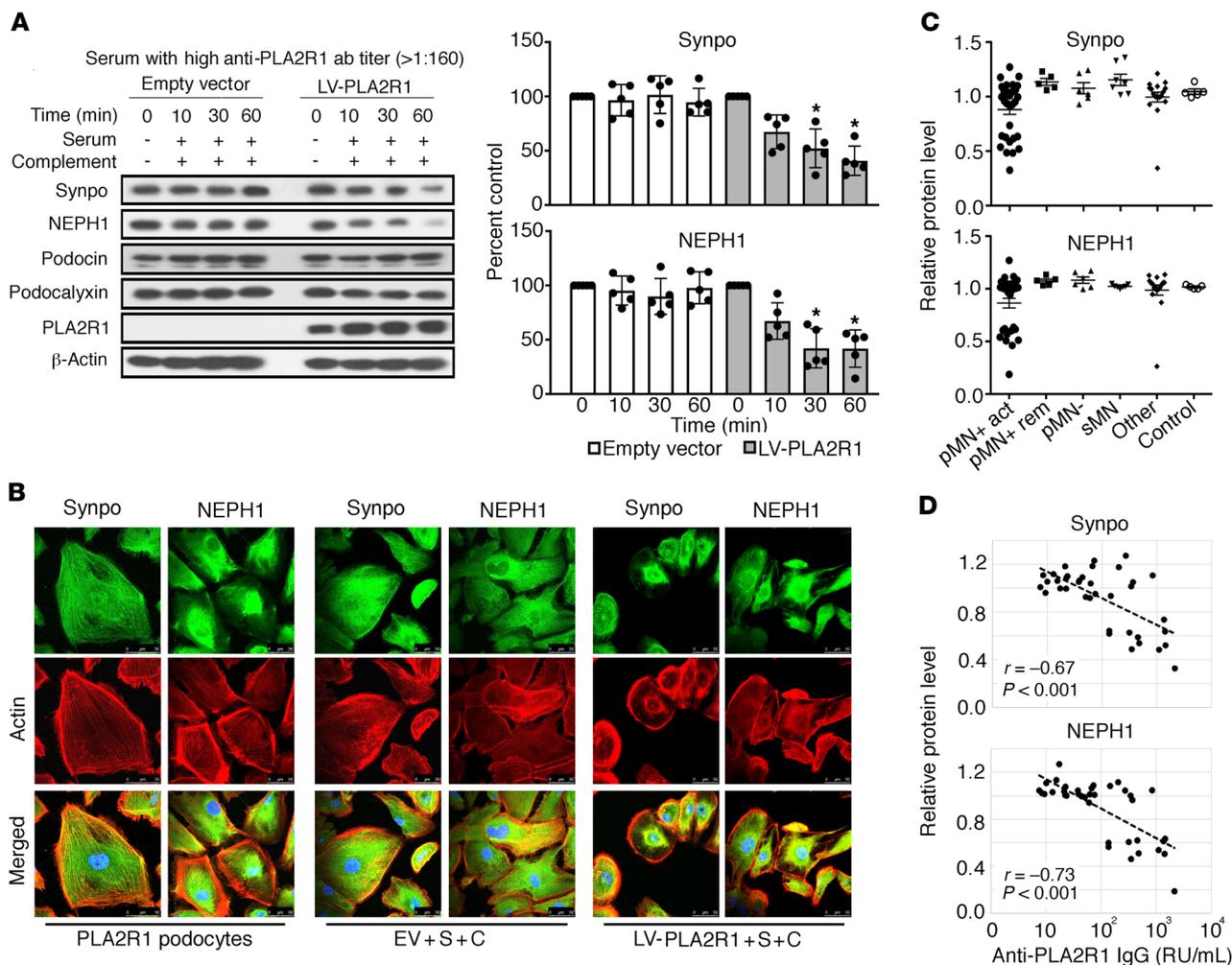
Figure 1. Anti-PLA2R1–positive sera induce complement-dependent degradation of synaptopodin and NEPH1. (**A**) Differentiated human podocytes infected with PLA2R1-containing lentivirus and control cells infected with empty vector were preincubated with 2.5% anti-PLA2R1–positive patient sera with high antibody titer (>1:160) for 30 minutes, treated for the indicated time periods with 5% NHS as a complement source, and analyzed by Western blotting against the indicated proteins. Bars represent mean ± SEM of the average of 3 independent experiments in each of 5 patients, *$P < 0.05$ by 1-way ANOVA and Tukey's post hoc test for the comparison with $t = 0$. (**B**) Immunofluorescence analysis of synaptopodin, NEPH1, and actin fibers in the same assay with serum from a patient with an anti-PLA2R1 titer of 451 RU/mL. The representative images were captured using a Leica SP8 upright confocal microscope and 63× objective lens. (**C**) The results were confirmed in a large cohort of anti-PLA2R1–positive pMN patients (pMN+) with active disease or in remission (act/rem), anti-PLA2R1–negative pMN patients (pMN–), secondary membranous nephropathy (sMN), other glomerular diseases (other), and healthy controls. Shown are synaptopodin and NEPH1 levels after preincubation with serum and 60 minutes of NHS exposure. Note that 1 patient with focal segmental glomerulosclerosis (group "other") showed a reduction of synaptopodin and NEPH1 that was not dependent on PLA2R1 expression (Supplemental Figure 10). (**D**) Correlation of synaptopodin and NEPH1 levels with ELISA-based anti-PLA2R1 antibody concentrations of patient sera used in the assay. *r*, Pearson's correlation coefficient; *$P < 0.05$.

ulosclerosis, but this was not dependent on PLA2R1 expression (Supplemental Figure 10).

Anti-PLA2R1 IgG4 activates complement through the lectin pathway. In gelatin veronal buffer containing calcium and magnesium, which is required for complement activation through the classical and lectin pathway, podocytes consistently showed a significant decrease in synaptopodin and NEPH1 levels (Figure 2A). Addition of recombinant human MBL led to a further decrease in synaptopodin and NEPH1 levels, whereas depriving calcium ions by using Mg^{2+}/EGTA buffer, which inhibits the classical and the lectin but not the alternative pathway, protected synaptopodin and NEPH1 from complement-induced degradation (Figure 2A). These results suggest a relevant role of the lectin pathway. We

therefore used SGMI-1 and SGMI-2 (12), 2 monospecific inhibitors of MASP-1 and -2, to selectively block the lectin pathway. Addition of either SGMI-1 or -2 effectively rescued synaptopodin and NEPH1 from degradation, clearly indicating a major role of the lectin pathway (Figure 2B).

Although anti-PLA2R1 autoantibodies in pMN are primarily of the IgG4 subclass, which is generally considered not to bind and activate complement, other IgG subclasses are also present to a lesser extent (13). To determine whether IgG4 was necessary and sufficient for the observed effect on podocytes, we used purified IgG4 from 3 high-titer anti-PLA2R1–positive patient sera for the complement assay (Supplemental Figure 11). Purified IgG4 bound to the surface of nonpermeabilized PLA2R1-expressing
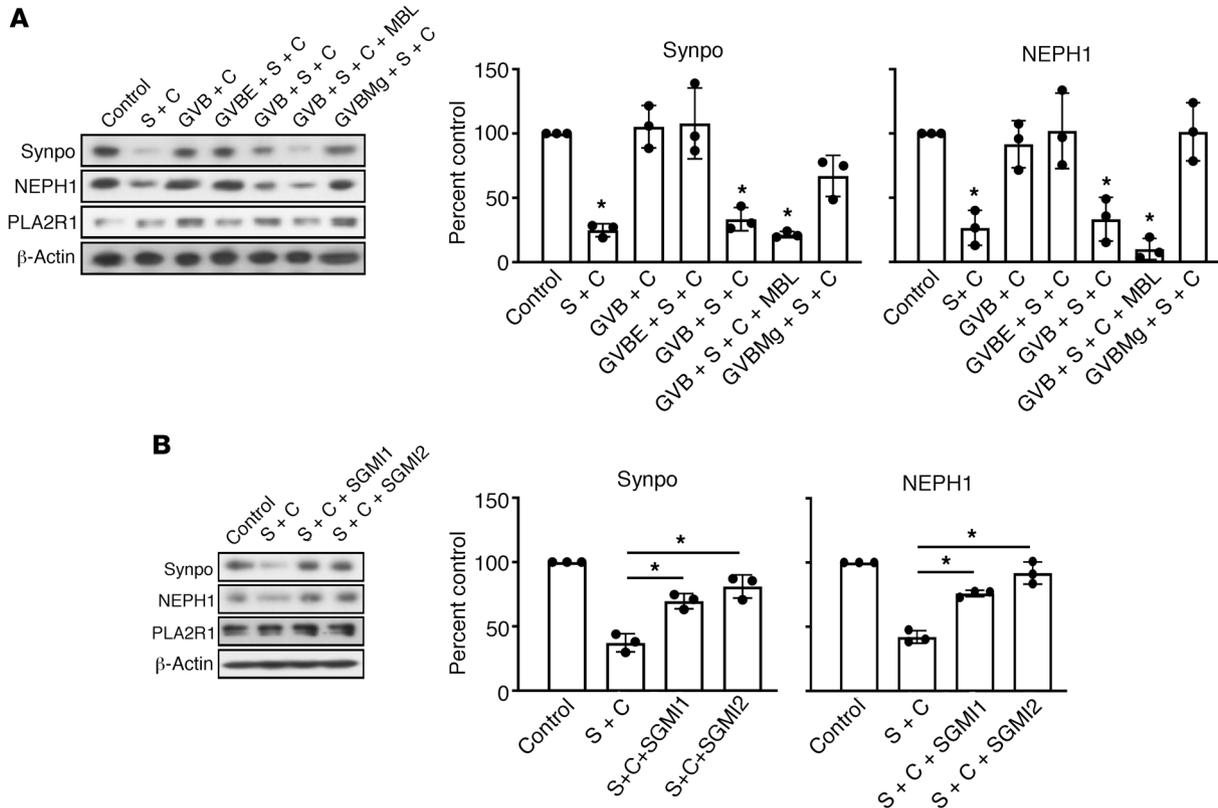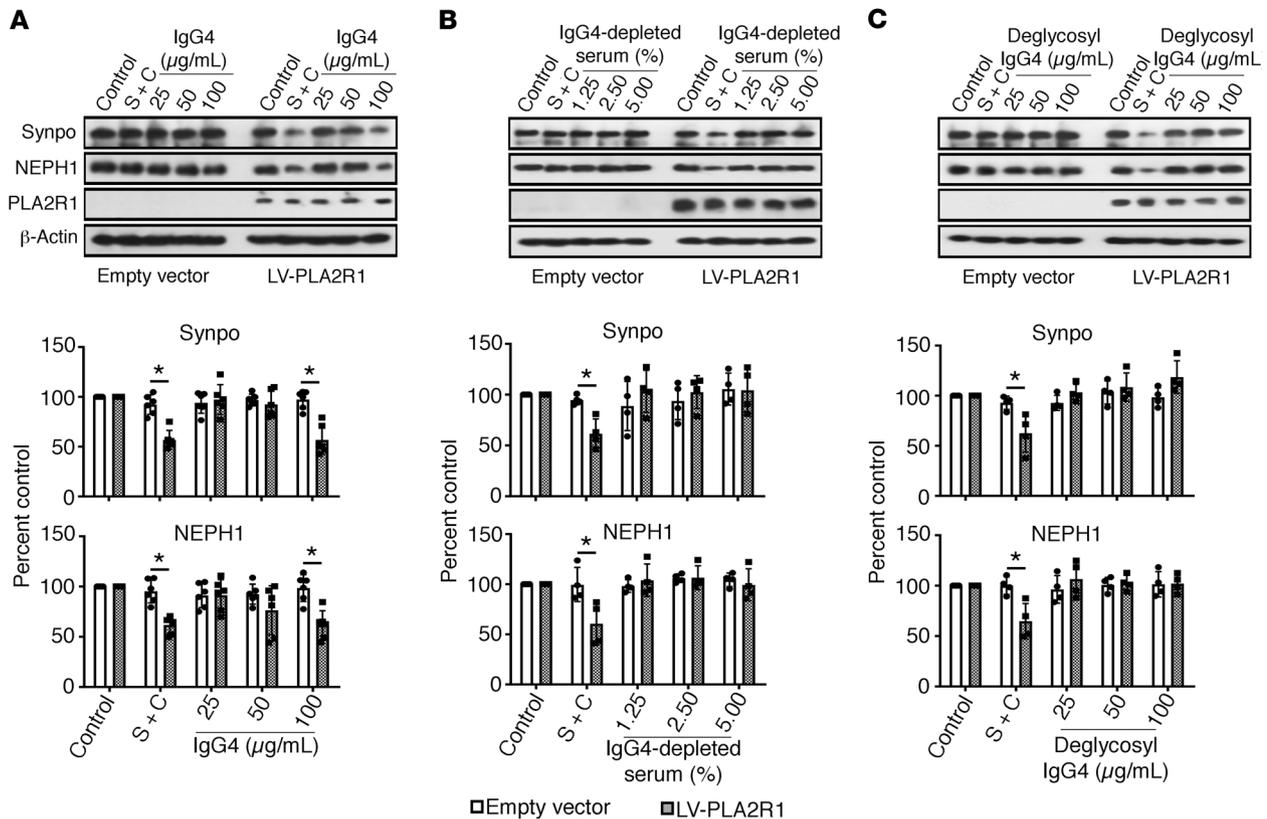
Figure 2. Degradation of synaptopodin and NEPH1 depends on the lectin pathway. (**A**) Podocytes expressing PLA2R1 were treated for 60 minutes with 5% NHS after preincubation for 30 minutes with 2.5% high-titer (1:1000, 2138 RU/mL) anti-PLA2R1–positive patient serum in incomplete RPMI1640 medium (second lane) or various gelatin veronal buffers (GVB). EDTA (GVBE) inhibits all complement pathways by depleting calcium and magnesium; addition of recombinant MBL in the presence of calcium and magnesium further facilitates activation of the lectin pathway, and calcium depletion with EGTA in the presence of magnesium (GVBMg) inhibits the classical and the lectin pathway but allows for activation of the alternative complement pathway. S = serum, C = complement. (**B**) The same experiment was performed in the presence of SGMI1 and SGMI2, specific inhibitors of the 2 proteases required for activation of the lectin pathway, MASP1 and MASP2, respectively. Bars represent mean ± SEM of 3 independent experiments, *$P < 0.05$ by 1-way ANOVA and Tukey's post hoc test for the comparison with control (**A**) or with S + C (**B**).

podocytes and showed perfect colocalization with PLA2R1 (Supplemental Figure 12), confirming cell surface expression of PLA2R1 and the PLA2R1 reactivity of purified IgG4. Whereas purified IgG4 induced complement deposition as well as synaptopodin and NEPH1 degradation, IgG4-depleted anti-PLA2R1 serum (which lost its reactivity against PLA2R1 in the ELISA) fixed only low levels of complement on podocytes and did not induce synaptopodin and NEPH1 degradation (Figure 3, A and B, Supplemental Figure 13).

Complement activation by anti-PLA2R1 IgG4 is glycosylation dependent. Immunoglobulins are posttranslationally modified by N-glycosylation. N-linked glycans attached to the conserved asparagine 297 of each CH2 domain of human IgG are important modulators of IgG effector functions (26). In rheumatoid arthritis, galactose-deficient IgG glycoforms have been shown to directly bind MBL (17). We therefore hypothesized that activation of the lectin pathway by anti-PLA2R1 IgG4 might be glycosylation dependent. Indeed, after deglycosylation, IgG4 from pMN patients no longer induced complement-mediated synaptopodin and NEPH1 degradation (Figure 3C) despite preserved immunoreactivity against PLA2R1 (Supplemental Figure 14). Immunofluorescence analyses revealed that total serum or isolated IgG4 from

anti-PLA2R1–positive pMN patients induced deposition of MBL and of complement C4d and C5b-9, and they reduced levels of synaptopodin and NEPH1 and triggered actin rearrangement. In contrast, deglycosylated IgG4 or serum depleted of IgG4 did not fix MBL on cells, did not affect synaptopodin and NEPH1 levels, and did not interfere with actin stress fibers, although some C4d and C5b-9 deposition was still detectable. SGMI-1 and -2 expectedly did not interfere with MBL binding but reduced downstream complement deposition on cells and rescued synaptopodin, NEPH1, and actin stress fibers (Figure 4).

MBL directly binds to anti-PLA2R1–positive IgG4. We first tested for direct binding of MBL to anti-PLA2R1 IgG4 by ELISA. Total IgG4 from pMN patients bound substantially more MBL than control IgG4, and MBL binding was inhibited by mannose (Supplemental Figure 15). Next, affinity-purified PLA2R1-specific IgG4 from 4 pMN patients was gel electrophoresed under reducing and nonreducing conditions and subjected to far-Western blot analysis with MBL using total IgG4 from healthy subjects as controls. MBL specifically bound to intact anti-PLA2R1 IgG4 (nonreducing conditions) and to its heavy chain (reducing conditions) but not to control IgG4 (Figure 5, A and B). Prior deglycosylation of anti-PLA2R1 IgG4 partially abolished MBL binding (Figure 5C).
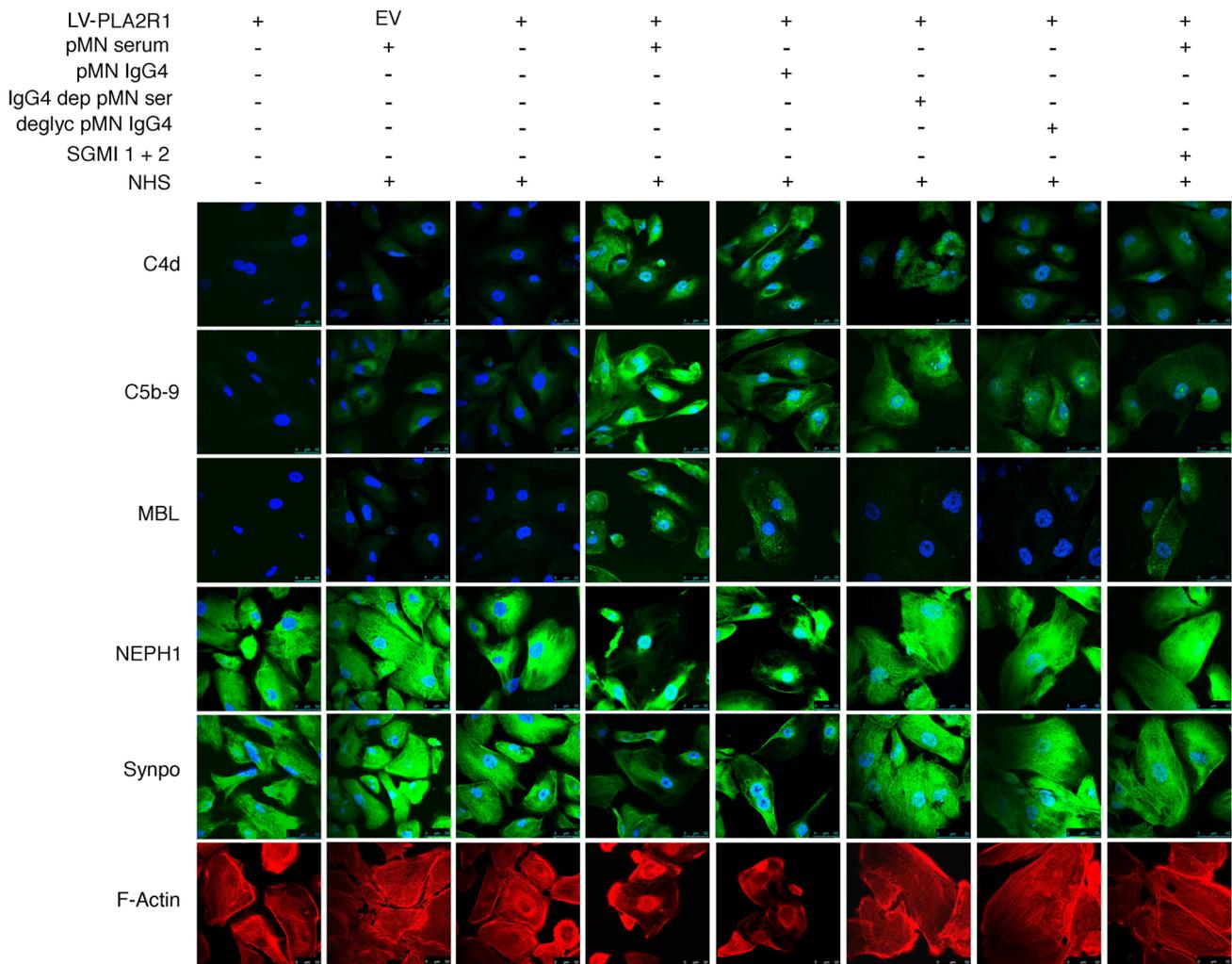
Figure 3. The effect of pMN serum on synaptopodin and NEPH1 depends on IgG4 and is glycosylation dependent. Human podocytes expressing PLA2R1 were treated for 60 minutes with 5% NHS after preincubation for 30 minutes with 2.5% whole serum from patients with high-titer anti-PLA2R1 antibodies (451 and 2138 RU/mL), with purified IgG4 from the same patients in the indicated concentration (**A**), with IgG4-depleted sera from the same patients (**B**), or with deglycosylated IgG4 (**C**). The concentration of IgG4 in 2.5% whole serum was 30 μg/mL. The bars represent mean ± SEM from 6 (**A**) or 4 (**B** and **C**) experiments in 2 patients, *$P < 0.05$ by Mann-Whitney U test for the comparison of LV-PLA2R1 to empty vector.

To determine whether MBL binding to anti-PLA2R1 IgG4 supports the activation of complement via the lectin pathway in vitro, affinity-purified anti-PLA2R1–specific IgG4 autoantibodies from 4 pMN patients and IgG4 from 4 healthy controls were immobilized on ELISA plates and incubated with NHS as a source of MBL and MASPs. Purified human C4 was added to increase the sensitivity of the assay, and the classical pathway was inactivated with 1 M NaCl, which disrupts the interaction between IgG and C1q (27). C4 activation was measured by the deposition of C4b. Anti-PLA2R1–specific IgG4 autoantibodies generated substantially and significantly more C4b than normal IgG4 (Figure 5D).

IgG4 antibodies from patients with pMN exhibit an altered glycosylation pattern. Alterations in the glycosylation profile of human IgG have been reported in several autoimmune diseases and affect the effector functions of IgG (26, 28). We therefore analyzed the glycosylation pattern of IgG4 isolated from pMN patients and controls. In a preliminary analysis, IgG4 from 4 pMN patients with high anti-PLA2R1 antibody titers (≥1:320 by immunofluorescence) showed a significant increase of the galactose-deficient G0F isoform with a corresponding decrease of galactosylated isoforms (Figure 6A). These results were confirmed in a larger cohort of patients with primary or secondary forms of membranous nephropathy, age- and sex-matched healthy controls, and patients with other glomerular diseases.

We found an increase in the relative amount of the galactose-deficient G0F and G0FN isoforms with a concomitant decrease in the G1F and G2F isoforms, which was more pronounced in pMN patients with a positive result in the cellular complement assay (Figure 6B). The relative amounts of the most abundant glycan isoforms in the various disease groups as well as derived traits (amount of galactose-deficient IgG4, overall galactosylation of diantennary glycans, bisection of diantennary glycans, and sialylation of diantennary glycans) according to age are shown in Supplemental Figures 17–24.

We next isolated anti-PLA2R1–specific IgG4 from the pooled serum of 4 patients and analyzed their glycosylation pattern. Compared with pooled total IgG4 from these patients, the observed alterations in glycosylation were more pronounced in the antigen-specific IgG4 fraction (Figure 6C). However, the altered glycosylation pattern appears to be a field-effect not specific for anti-PLA2R1 IgG4 nor for IgG4, since total IgG1 and IgG2 from pMN patients exhibited similar but slightly less pronounced alterations (Supplemental Figure 25). Notably, the IgG4 glycosylation pattern correlated with anti-PLA2R1 antibody levels and with the degree of synaptopodin and NEPH1 degradation induced by these sera in the cellular complement assay (Figure 6, D–F and Supplemental Figure 26) and tended to correlate with proteinuria, although this was not statistically significant (Supplemental Figure 27).

|								
LV-PLA2R1	+	EV	+	+	+	+	+	+
pMN serum	-	+	-	+	-	-	-	+
pMN IgG4	-	-	-	-	+	-	-	-
IgG4 dep pMN ser	-	-	-	-	-	+	-	-
deglyc pMN IgG4	-	-	-	-	-	-	+	-
SGMI 1 + 2	-	-	-	-	-	-	-	+
NHS	-	+	+	+	+	+	+	+

Figure 4. Immunofluorescence analysis of complement deposition, synaptopodin and NEPH1 expression, and actin fibers under various experimental conditions. Human podocytes infected with PLA2R1-containing lentivirus (LV-PLA2R1) or empty virus (EV) were treated with 2.5% high-titer (451 RU/mL) anti-PLA2R1–positive pMN serum (pMN serum); isolated total IgG4 from the same patient (pMN IgG4) at a final concentration of 100 μg/mL (with an antibody level of 1295 RU/mL in the ELISA at a concentration of 8 mg/mL); IgG4-depleted serum from the same patient (IgG4 dep pMN ser), which had no residual reactivity against PLA2R1 (4 RU/mL; cut off for positivity 20 RU/mL); deglycosylated IgG4 from the same patient (deglyc pMN IgG4); or patient serum in the presence of SGMI 1 and 2, both at a concentration of 20 μM (SGMI 1 + 2); and/or 5% NHS as a source of functional complement, as indicated above. The cells were then fixed, permeabilized, and stained for C4d (green), C5b-9 (green), MBL (green), NEPH1 (green), synaptopodin (green), and actin (red). The representative images were captured using a Leica SP8 upright confocal microscope and 63× objective lens.

Complement effector pathways in pMN. Activation of complement through any of the 3 activation pathways eventually triggers the formation of the membrane attack complex (MAC) — consisting of the complement component C5b-9 — and the generation of the anaphylatoxins C3a and C5a, which signal through cell surface receptors. In cultured rodent podocytes, sublytic complement injury induced by non-IgG4 antibodies directed against target antigens unrelated to PLA2R1 is mediated through C5b-9 insertion in cell membranes and subsequent calcium influx that leads to activation of several signaling pathways (21). Likewise, in our cellular model, synaptopodin and NEPH1 were rescued when we used C6-deficient serum as a source of complement (Figure 7A), confirming that MAC assembly was required to induce their cleavage. We next tested whether the anaphylatoxins C3a and C5a are also involved in anti-PLA2R1–mediated podocyte injury. Cultured human podocytes expressed the complement receptors CR4, C3aR1, C5aR1, and C5L2 but not CR1, CR2, or CR3 (Supplemental Figure 28). Although individual gene silencing of any of these receptors did not protect podocytes (Supplemental Figure 28, C and D), combined gene silencing of C3aR1 and C5aR1 resulted in substantial protection of podocytes from sublytic complement–mediated injury, as did the inhibition of these receptors by small molecule inhibitors (Figure 7, B and C). Hence, activation of C3aR1 and/or C5aR1 along with C5b-9 insertion is required for anti-PLA2R1– and complement-mediated degradation of synaptopodin and NEPH1.

Interestingly, there was an increased expression of C5aR1 in vitro after exposing the podocytes to pMN sera and complement (Supplemental Figure 29). In vivo, we observed increased expression of C3aR1 and C5aR1 in archived biopsy samples of PLA2R1-positive pMN patients (Figure 8, A and B and Supplemental Figure 30). The increased expression was more pronounced
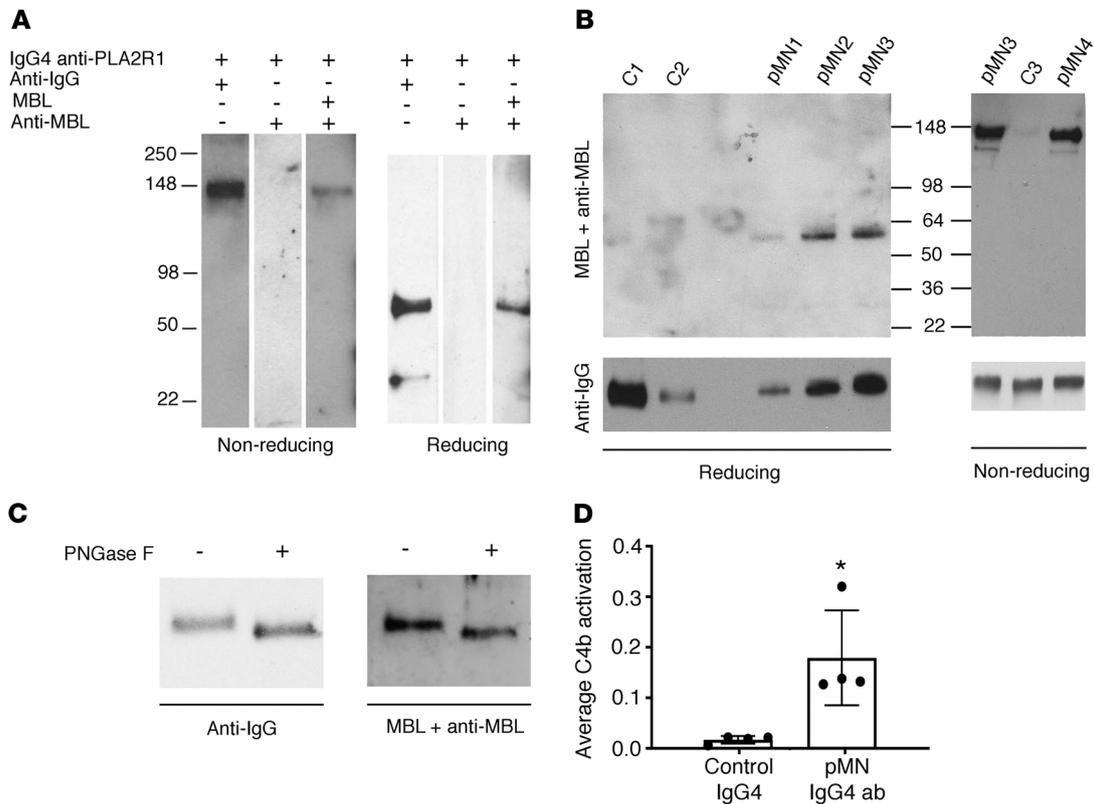
Figure 5. Anti-PLA2R1–specific IgG4 directly binds MBL and triggers lectin pathway activation. (**A**) Affinity-purified anti-PLA2R1–specific IgG4 from a patient with pMN was resolved by SDS-PAGE under nonreducing and reducing conditions, blotted, and stained for human IgG or MBL with or without prior incubation with recombinant MBL, as indicated. (**B**) MBL binding was confirmed using anti-PLA2R1–specific IgG4 from 4 additional pMN patients and total IgG4 from healthy controls. (**C**) The experiment was repeated with anti-PLA2R1–specific IgG4 with or without prior deglycosylation. The densitometric ratio of MBL to IgG staining was reduced by 64% through deglycosylation. (**D**) An ELISA plate was coated with anti-PLA2R1–specific or control IgG4, followed by the addition of NHS as a source of MBL and MASPs, human C4, and anti-C4b antibody either in the presence of 10 mM calcium or 1 mM EDTA. C4 deposition was calculated as the difference in OD in the presence versus absence of calcium divided by the amount of IgG4. The bars represent mean ± SEM for triplicate measurements in samples from 4 pMN patients and 4 controls; *$P < 0.05$ by Mann-Whitney U test.

in high-titer anti-PLA2R1–positive patients, although this correlation did not reach statistical significance (Supplemental Figure 31). In the same biopsy samples, we confirmed synaptopodin and NEPH1 reduction in pMN patients in vivo, and synaptopodin levels inversely correlated with PLA2R1 titer (Figure 8C). Further correlations are shown in Supplemental Figure 31; patient characteristics for the biopsy samples are in Supplemental Table 2.

Synaptopodin and NEPH1 are degraded by 2 distinct proteolytic pathways. Given the rapid reduction of synaptopodin and NEPH1 levels, we suspected a proteolytic mechanism. Synaptopodin has been previously shown to be degraded by cathepsin L upon calcineurin-dependent dephosphorylation in certain glomerular diseases (29). In line with being cleaved by cathepsin L, synaptopodin was rescued from complement-mediated degradation by the cysteine protease inhibitor E64 and the calcineurin inhibitor cyclosporine A (Figure 9, A and B). Although these compounds did not rescue NEPH1, pepstatin A (an aspartic proteinase inhibitor) specifically protected NEPH1 but not synaptopodin from degradation (Figure 9C). Thus, anti-PLA2R1 antibody–dependent complement injury of podocytes led to synaptopodin degradation via cathepsin L and to NEPH1 degradation via an aspartic protease. Since dynamin is another proteolytic target of cathepsin L in podocytes (30), we assayed

dynamin levels upon anti-PLA2R1– and complement-mediated damage in podocytes. Dynamin was degraded to a similar degree as synaptopodin and rescued by pretreatment of cells with E64 (Supplemental Figure 32).

Synaptopodin has been shown to be phosphorylated by protein kinase A (29), and C3aR1 and C5aR1 are G protein–coupled receptors that have been shown to inhibit cAMP production in dendritic cells (31, 32). We therefore tested whether cAMP levels were affected in our cellular model of pMN and observed a decrease of cAMP levels in podocytes upon addition of anti-PLA2R1–positive pMN serum and complement, which was prevented by inhibition of C3aR1 and C5aR1 (Figure 9D).

Discussion

In this study, we analyzed the molecular mechanisms of podocyte damage in anti-PLA2R1–associated pMN. We identified synaptopodin and NEPH1, 2 essential podocyte proteins, as the targets of complement-induced podocyte injury. An altered glycosylation pattern of IgG4 was identified in pMN patients that facilitated complement activation through the lectin pathway.

A large body of evidence points to a central role of complement in the pathogenesis of pMN (13). However, the identity of the complement activation pathways and the complement effec-
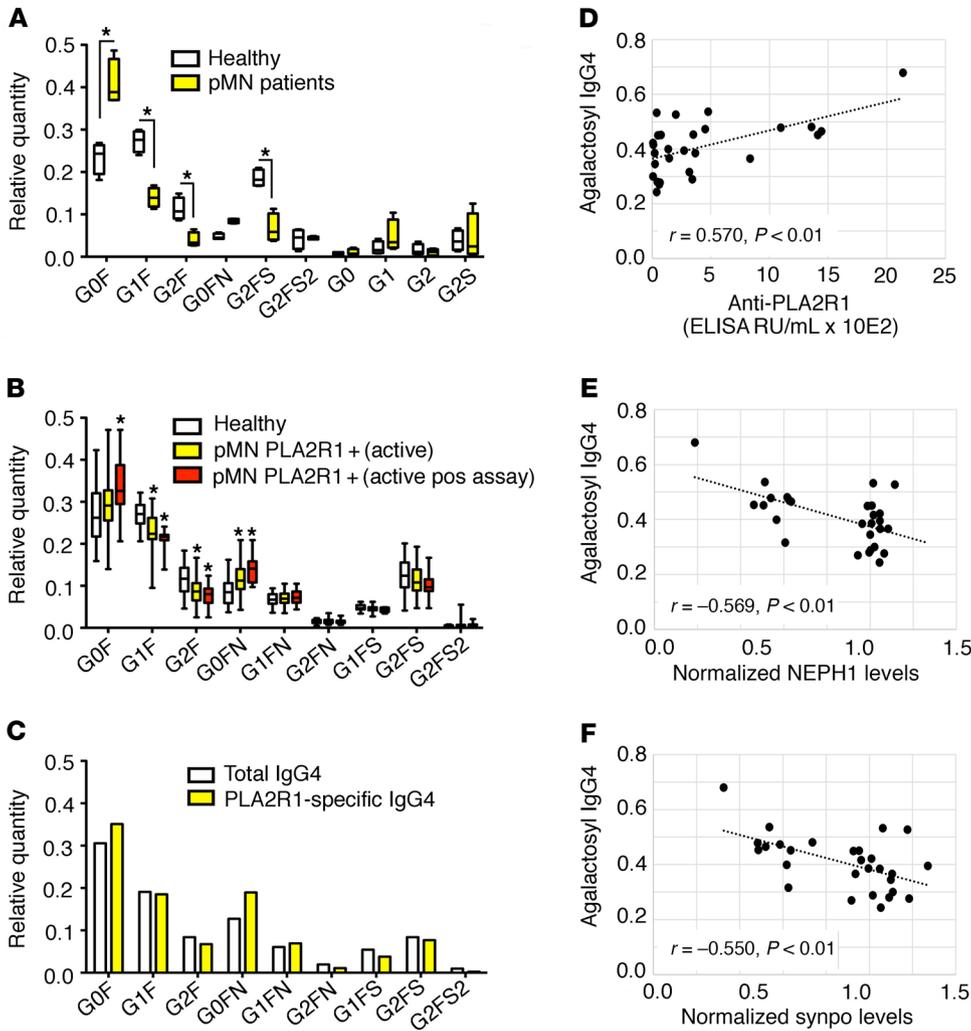
Figure 6. IgG4 antibodies from patients with pMN exhibit an altered glycosylation pattern. (**A**) Preliminary analysis of the glycosylation pattern of IgG4 purified from sera of pMN patients and controls ($n = 4$ each). The box shows median and IQR, the whiskers minimum and maximum values, *$P < 0.05$ unpaired t test. (**B**) Analysis of the IgG4 glycosylation pattern using nanoLC-MS of glycopeptides in an extended cohort. The entire cohort of PLA2R1-positive pMN patients with active disease ($n = 31$, for definition of active disease see Supplemental Table 2) and patients with a positive result (i.e., a statistically significant decrease of synaptopodin and NEPH1 by more than 25% in 3 independent experiments) in the cellular complement assay ($n = 10$) were compared with age- and sex-matched healthy controls ($n = 39$). The box shows median and IQR, the whiskers minimum and maximum values, *$P < 0.05$ adjusted for residual confounding by differences in age and sex. (**C**) PLA2R1-specific IgG4 was purified from the pooled IgG4 fraction of 5 pMN patients (with anti-PLA2R1 levels of 451–1443 RU/mL) and the glycosylation pattern was compared with total IgG4 from these patients. (**D**) Correlation of the fraction of agalactosyl IgG4 (G0F + G0FN/total IgG4) with anti-PLA2R1 antibody levels, (**E**) with synaptopodin, and (**F**) with NEPH1 levels after exposure to patient sera and complement in all patients with active pMN. r, Pearson's correlation coefficient. See Supplemental Figure 16 for an explanation of the glycosyl side chain nomenclature.

tor mechanisms involved have remained elusive. Paradoxically, the predominant subclass of anti-PLA2R1 antibodies in pMN is IgG4 (11), which is considered unable to activate complement. In our cellular assay, IgG4 depletion of pMN patient serum led to complete protection of synaptopodin and NEPH1 from degradation. On the other hand, IgG4 purified from anti-PLA2R1–positive patient sera was sufficient to induce complement deposition as well as degradation of synaptopodin and NEPH1. The concentration of purified IgG4 to achieve this effect was somewhat higher than that of IgG4 in the assay performed with whole patient serum.

On the other hand, IgG4-depleted serum did not elicit any effect even when applied in higher concentrations and did not retain any reactivity against PLA2R1. This suggests either a synergistic effect of other serum components or a partial loss of complement-activating capacity of IgG4 during the isolation process; we confirmed that the antigen recognition was preserved. A contributing effect of other IgG subclasses in some patients cannot be excluded, but taken together, our data showed that IgG4 is capable of inducing complement activation and podocyte damage and is likely not only the predominant isotype of anti-PLA2R1 antibodies but also primarily responsible for podocyte damage.

It has been proposed previously that complement activation in pMN might proceed via the lectin pathway (13), but definitive experimental evidence for this hypothesis has not yet been published. Previous data supporting the role of the lectin pathway in pMN include the observation of MBL deposition in membranous nephropathy biopsies (8, 15, 16) and the fact that C4 is generally present in the absence of C1q in glomerular immune complexes in pMN (8–10). The lectin complement pathway is usually initiated when a pattern recognition molecule (PRM) binds to a carbohydrate motif (a pathogen-associated pattern) present on invading microorganisms or to endogenous ligands displaying damage-associated patterns upon cell damage, cell stress, and inflammation. One of the PRMs of the lectin pathway is MBL. We observed that adding recombinant MBL increased complement-mediated damage of the podocytes, while specific inhibition of the key lectin pathway activators MASP-1 and -2 by the small protein inhibitors SGMI-1 and SGMI-2 (12) blocked complement activation and protected podocytes from synaptopodin and NEPH1 degradation. These inhibitors, as expected, did not interfere with MBL binding to cells. Thus, the lectin pathway appears to be instrumental for podocyte injury in pMN. As demonstrated by ELISA and far-Western blot experiments, anti-PLA2R1 IgG4 directly bound MBL in a calcium-dependent manner, supporting a direct activation of the lectin pathway by anti-PLA2R1 IgG4.
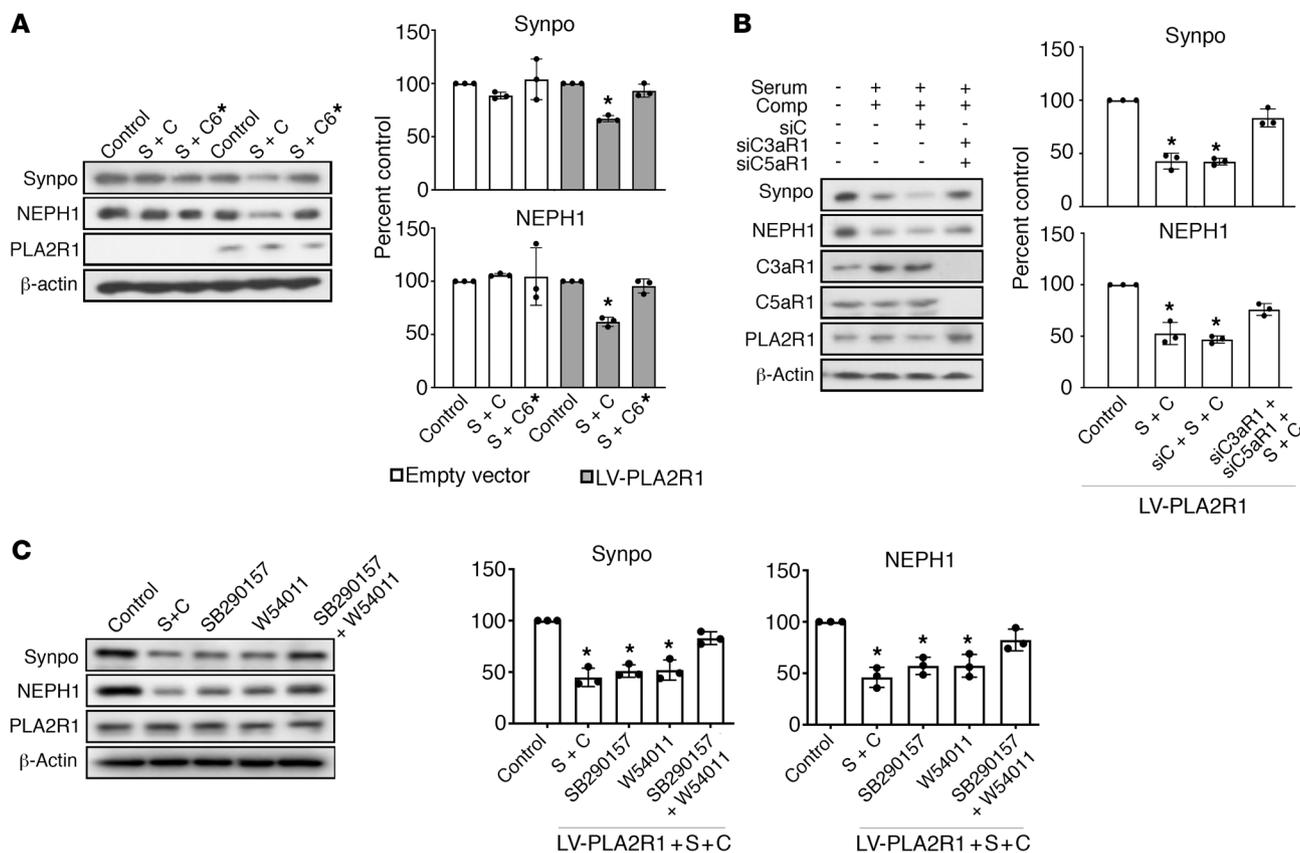
Figure 7. Complement effector pathways in pMN. (A) Differentiated human podocytes expressing PLA2R1 were preincubated with 2.5% high-titer (1:1000, 2138 RU/mL) anti-PLA2R1–positive membranous nephropathy serum followed by exposure to 5% NHS (S + C) or C6-deficient human serum (S + C*) for 1 hour. **(B)** The same experiment was performed with NHS in podocytes after siRNA-mediated combined knockdown of C3aR1 and C5aR1 (siC3aR1 + SiC5aR1 + S + C) or control siRNA (siC + S + C). **(C)** The same experiment performed with serum from a patient with high-titer (451 RU/mL) anti-PLA2R1 antibodies in the presence or absence of small-molecule C3aR and C5aR antagonists (SB290157 and W54011, respectively). The bars represent mean ± SEM; *$P < 0.05$ by 1-way ANOVA and Tukey's post hoc test for the comparison with control.

Further supporting the role of the lectin pathway in anti-PLA2R1–associated pMN, MBL and MASP-1 serum levels were previously observed to be higher in PLA2R1-positive versus PLA2R1-negative pMN patients and inversely correlated with the chance of achieving complete remission (33). On the other hand, 5 pMN patients with genetic MBL deficiency have been reported (34). The fact that pMN can also develop in people with MBL deficiency needs to be interpreted by taking into account that MBL represents only one of several PRMs that activate the lectin pathway: collectins (including MBL, collectin-L1, and collectin-K1) and ficolins (ficolin-1, -2, and -3). These other PRMs also bind acetylated sugars and may participate in IgG4-induced complement activation even in MBL-deficient pMN patients. Nevertheless, MBL deficiency should dampen the level of lectin pathway activation, and in fact, the authors also reported an altered pattern of immunofluorescence staining (34), showing less C4d but stronger C3 deposition in the glomeruli of these MBL-deficient patients compared with other patients with pMN. This suggests that in the context of a reduced lectin pathway capacity, the alternative complement pathway becomes more active in pMN.

Alterations in the glycosylation pattern of IgG have been described in various diseases, including autoimmune disorders

and cancer, as well as in aging (26, 28, 35), affecting their pro- and antiinflammatory properties. In rheumatoid arthritis, loss of galactose has been suggested to make the 4-OH group of GlcNAc accessible for lectin binding and thus render IgG molecules capable of activating complement via the lectin pathway (17). Here, we found that IgG4 from anti-PLA2R1–positive pMN patients exhibited an altered glycosylation pattern. In particular, the proportion of galactose-deficient IgG4 glycoforms was increased and the galactose deficiency of IgG4 correlated with anti-PLA2R1 antibody titer as well as synaptopodin and NEPH1 degradation in the cellular assay. Although the alterations in the glycosylation pattern appeared to be particularly prominent on PLA2R1-specific IgG4, they were neither specific to PLA2R1-specific autoantibodies, nor to IgG4 as compared with IgG1 and 2, nor to pMN as compared with other glomerular diseases. In line with previous observations (36), we also noticed a relevant effect of age. Notably, the alterations in anti-PLA2R1–positive pMN patients compared with age-matched controls were particularly prominent in young patients. Taken together, these data suggest that altered glycosylation might render anti-PLA2R1 autoantibodies of the IgG4 subtype capable of activating the complement system. In support of this hypothesis, deglycosylation of IgG4 protected synaptopodin and NEPH1 in the cellular assay, abrogated MBL and complement fix-
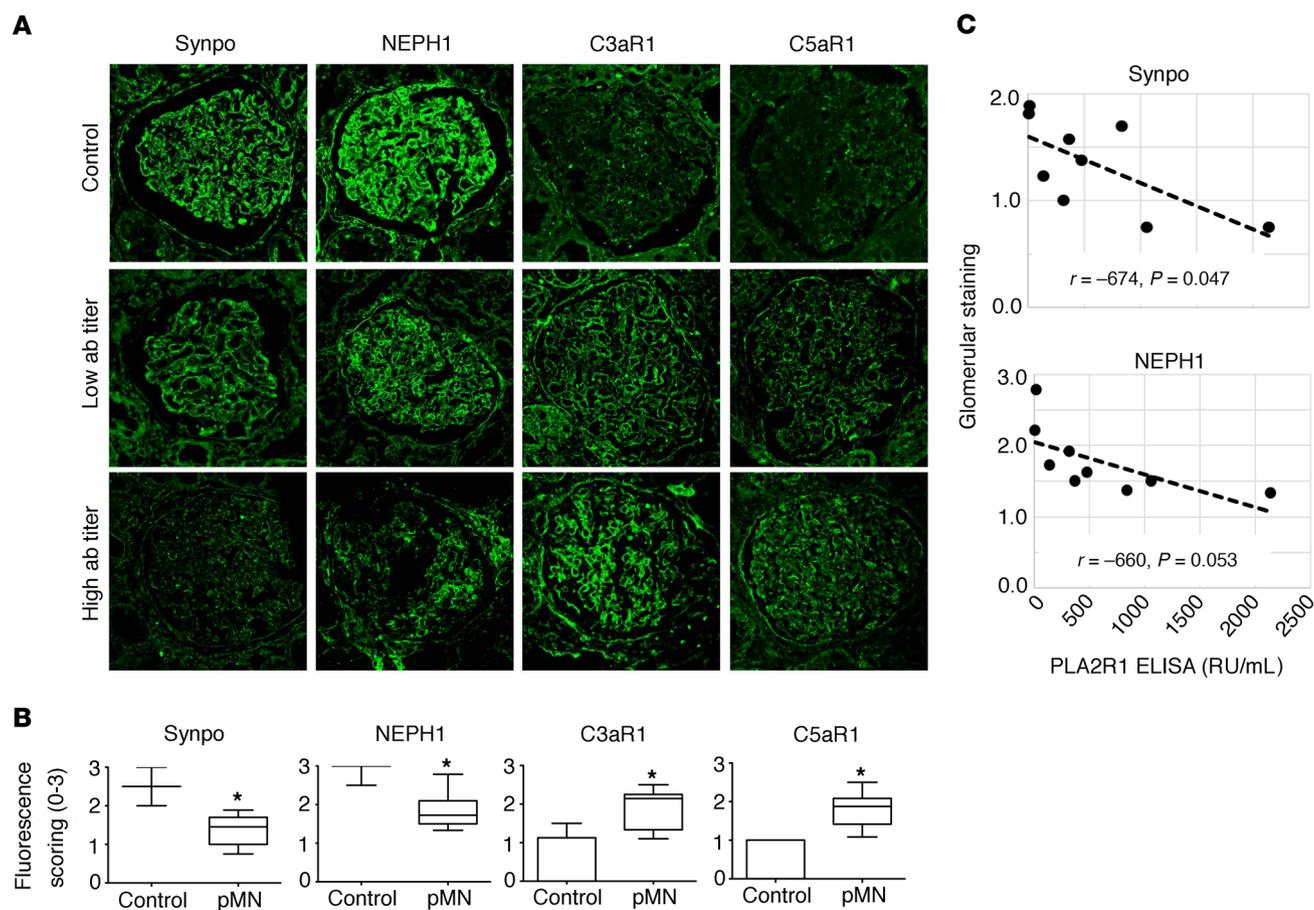
Figure 8. Expression of complement receptors and loss of synaptopodin and NEPH1 in human pMN biopsies. (**A**) Representative biopsy slides of normal human kidney tissue and patients with anti-PLA2R1–associated pMN stained for synaptopodin, NEPH1, C3aR1, and C5aR1. The images were captured using a Leica SP8 upright confocal microscope and 63× objective lens. (**B**) The expression levels of synaptopodin and NEPH1 are significantly decreased in anti-PLA2R1–positive pMN patients, while expression of C3aR1 and C5aR1 was increased as compared with control kidney tissue (n = 11 biopsies from 10 patients with pMN, see Supplemental Table 2, 2–10 glomeruli per patient vs. 14 control glomeruli from different individuals). The bars represent mean ± SEM, *P < 0.05 by Mann-Whitney U test. (**C**) Glomerular synaptopodin and NEPH1 staining was compared with anti-PLA2R1 antibody levels where available.

ation on podocytes, and strongly reduced direct binding of MBL in the far-Western blot analysis.

Activation of the complement system through any of the 3 activation pathways led to assembly of the MAC (C5b-9) as well as the generation of the anaphylatoxins C3a and C5a. Complement-dependent podocyte injury in membranous nephropathy has been primarily attributed to C5b-9 (21). The complement receptors C3aR1 and C5aR1 are expressed mainly on leukocytes and are known for their chemotactic and activating effect on these cells. Here, we showed that C3aR1 and C5aR1 are expressed on podocytes and that their expression is induced during human pMN in vivo. Increased C3aR1 expression has also been recently reported in rodent models of diabetic nephropathy (37), suggesting that our observation might not be specific to pMN. Concurrent blockade of both receptors rescued a decrease in cAMP that we observed as a response to pMN serum and complement and ameliorated complement-induced podocyte injury. As previously shown in other models, C6 deficiency also protected podocytes from damage. Hence, MAC insertion and activation of C3aR1 or C5aR1 appear to be involved in complement-mediated sublytic podocyte injury in anti-PLA2R1–associated pMN. It is noteworthy that we did not

detect expression of CR1 in our cultured podocytes, which has been reported to be expressed in vivo in podocytes (38, 39). Thus, we were not able to analyze a potential protective role of this complement regulatory protein.

Several cellular mechanisms of sublytic complement–induced podocyte damage have been described for rodent podocytes and non-IgG4 antibodies directed against antigens other than PLA2R1 (21, 40). To our knowledge, we report the first model of primary membranous nephropathy using PLA2R1-expressing human podocytes and human anti-PLA2R1 sera or isolated IgG4. As a cellular mechanism of podocyte damage, we identified 2 distinct proteolytic pathways that led to partial degradation of synaptopodin and NEPH1. Reduction of these proteins could be demonstrated in our in vitro model and in vivo in human biopsies from pMN patients. These 2 proteins are critical to maintaining podocyte structure and function (41–43) and their reduction was associated with alterations in the actin cytoskeleton in our model. The actin cytoskeleton is critical in maintaining podocyte foot process integrity, and loss of actin stress fibers is associated with foot process effacement and proteinuria in vivo (44). Cleavage of synaptopodin by cathepsin L has been demonstrated as a mecha-
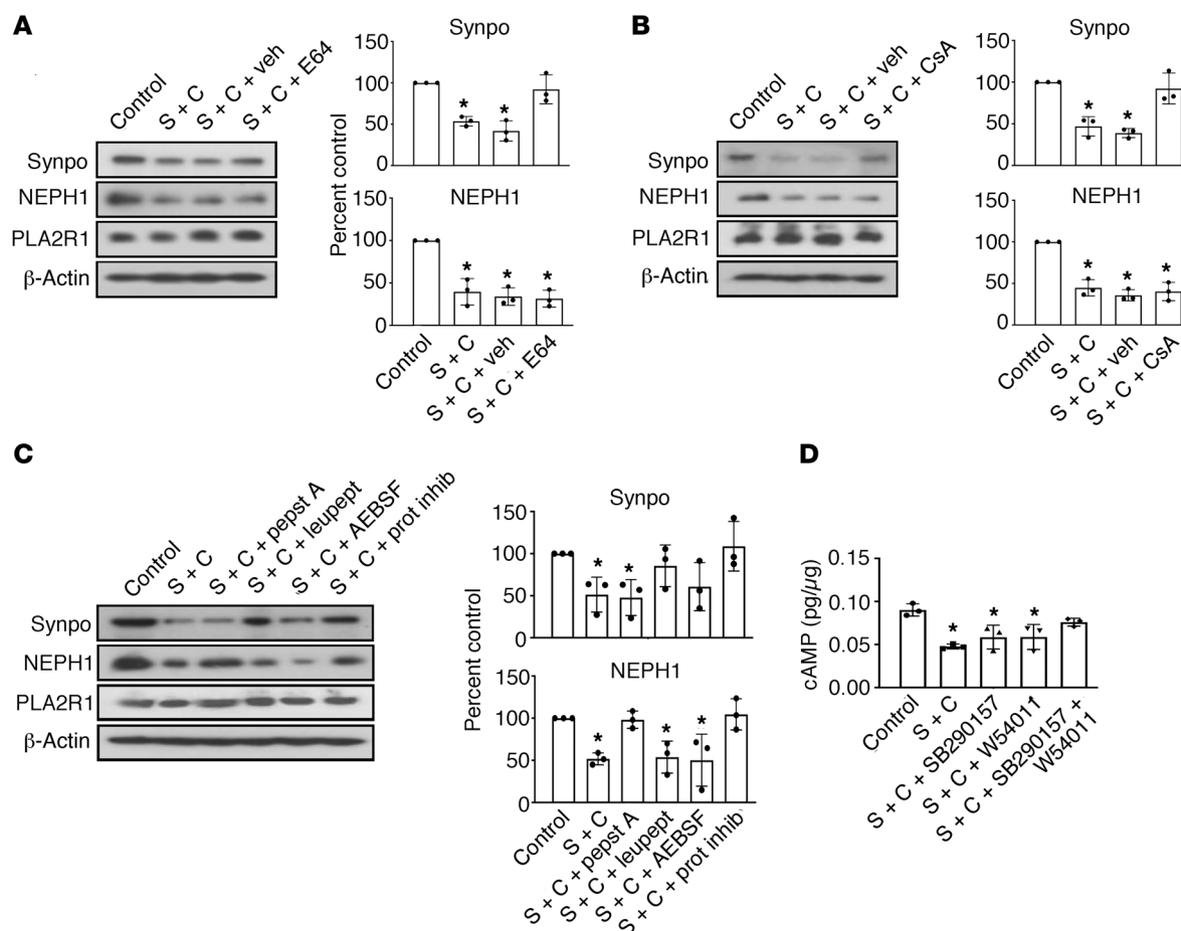
Figure 9. Determination of proteases involved in synaptopodin and NEPH1 degradation. (**A**) Differentiated podocytes infected with PLA2R1-containing lentivirus were pretreated for 30 minutes with 2.5% high-titer (1:1000) anti-PLA2R1–positive human membranous nephropathy serum, followed by treatment for 60 minutes with 5% NHS as a source of complement (S + C) after pretreatment for 60 minutes with the cysteine protease inhibitor E64 (20 μM) or vehicle. (**B**) Same experiment performed with cyclosporine A (CsA, 1 μM). (**C**) Same experiment performed with various protease inhibitors, including pepstatin A (1 μM), leupeptin (1 mM), AEBSF (4-(2-Aminoethyl)benzenesulfonylfluoride) (0.25 mM), or 1 × protease inhibitor cocktail. (**D**) The same experiment was performed after pretreatment for 60 minutes with the C3aR and C5aR inhibitors SB290157 and W54011, respectively, either alone or combined, and cAMP levels were measured. n = 3 for all experiments, the bars represent mean ± SEM, *P < 0.05 by 1-way ANOVA and Tukey's post hoc test.

nism of proteinuria in several disease models (29), where protein kinase A–dependent phosphorylation protected synaptopodin and calcineurin-mediated dephosphorylation rendered it susceptible to cleavage. Our data are in good agreement with this model, since the calcineurin inhibitor ciclosporin A protected synaptopodin, as did C3aR1 and C5aR1 inhibition, which maintained normal cellular cAMP levels. Aspartic protease–mediated cleavage of NEPH1 has to our knowledge not been previously reported as a mechanism of glomerular diseases. We did not find any effect on podocin, which has been reported to be affected in passive and active Heymann nephropathy (45). As mentioned above, these rodent models of pMN do not recapitulate key features of human anti-PLA2R1–associated pMN and may include other cellular mechanisms. Furthermore, a particular advantage of our model is that it allows analysis of the very early effects of autoantibodies and complement on podocytes, which may affect numerous additional podocyte proteins at later stages, given their close interaction at the slit diaphragm.

Together, our data support a model for the pathogenesis of pMN in which 3 events contribute to podocyte damage (Figure 10): (a) the development of IgG4 autoantibodies against PLA2R1 (specific to the disease); (b) an altered glycosylation pattern of immunoglobulins (likely not specific to the disease) that renders IgG4 autoantibodies capable of activating complement through the lectin pathway; and (c) upregulation of the complement receptors C3aR1 and C5aR1 (likely not specific to the disease), which facilitate anaphylatoxin signaling in podocytes. Formation of the MAC and C3aR1 or C5aR1 signaling converge in the proteolysis of synaptopodin and NEPH1, which are crucial to maintaining the podocyte actin cytoskeleton and the slit diaphragm, respectively.

Our findings have important therapeutic implications. Current treatments for pMN consist of initial nonimmunosuppressive therapy with angiotensin-converting enzyme inhibitors or angiotensin receptor blockers and immunosuppressive treatments in the case of severe disease or persistent nephrotic syndrome despite conservative treatment (46). Immunosuppressive treatments, which reduce the production of novel antibodies, bear a considerable potential for side effects and induce remission only with a delay of usually 6 to 12 months due to the persistence of previously deposited immune complexes. Thus, blockade of the lec-
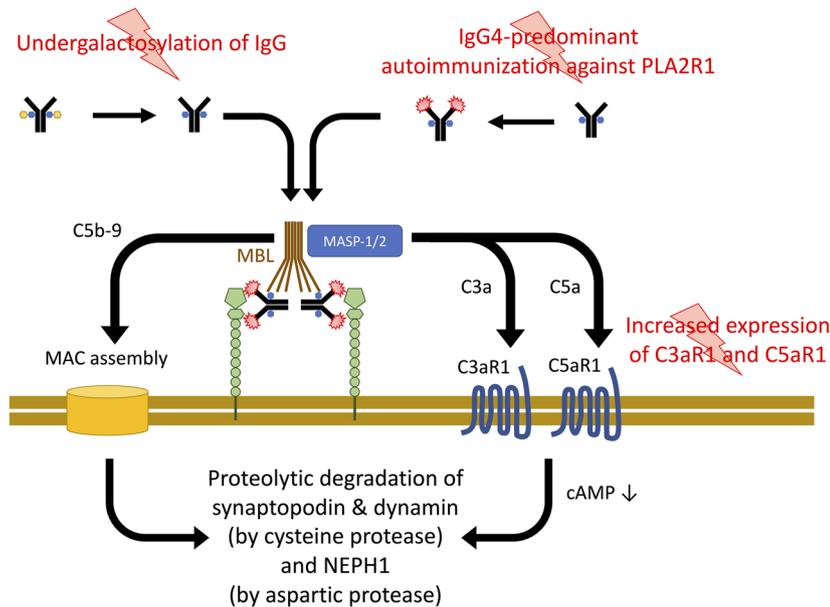
Figure 10. Three-hit model for the pathogenesis of PLA2R1-associated pMN. Through as yet unidentified triggers, IgG4-predominant immunization against PLA2R1 is induced. An alteration of glycosylation allows these antibodies, when bound to their target antigen, to bind MBL and to activate the lectin complement pathway. Complement activation leads to assembly of the membrane attack complex (MAC) and C3a and C5a generation. A third hit, increased C3aR1 and C5aR1 expression on podocytes, facilitates C3aR1 and C5aR1 signaling, which decreases cellular cAMP levels. C3aR1/C5aR1 signaling and MAC insertion converge in the proteolysis of synaptopodin, NEPH1, and dynamin.

tin pathway represents a potential approach to treat pMN, either as a substitute for or in conjunction with current immunosuppressive treatments. A specific MASP-2–targeting monoclonal antibody (narsoplimab, Omeros) is currently being evaluated in phase 2 clinical trials for a number of other renal and nonrenal diseases and has entered phase 3 testing for the treatment of IgA nephropathy. In IgA nephropathy, galactose deficiency of O-linked glycans on IgA1 has been shown to play an important pathogenic role (47). Furthermore, MBL is found in biopsies of IgAN patients, and in addition to inducing anti-IgA1 autoantibodies, galactose-deficient IgA1 in IgAN might bind MBL and other lectins, similar to what we have observed for IgG4 in pMN (48).

In conclusion, our study provides detailed insights into the mechanisms of complement activation and its effector pathways leading to podocyte injury in human anti-PLA2R1–associated pMN. Specifically, our data demonstrate that anti-PLA2R1 antibodies of the IgG4 isotype activate the complement system upon binding to podocyte PLA2R1 and that this effect is facilitated by an aberrant glycosylation that allows the activation of the lectin pathway by IgG4.

Methods

Human sera and kidney tissue. Human sera for the initial experiments were obtained from the biobank of the Division of Nephrology, University Hospital of Zurich. The biobank follows the International Society for Biological and Environmental Repositories Best Practices for Repositories, Collection, Storage, Retrieval and Distribution of Biological Materials for Research (49) and the OECD Guidelines for Human Biobanks and Genetic Research Databases, 2009 (50) (http://www.

oecd.org/science/biotech/44054609.pdf). Additional sera were provided by Uyen Huynh-Do and Michael Horn from the University Hospital of Bern and Helmut Hopfer from the University Hospital of Basel. Healthy control sera were obtained from the regional blood service of the Swiss Red Cross in Schlieren, Zurich, Switzerland.

Human kidney biopsy samples from patients with membranous nephropathy and patients with other diseases were obtained from the biobank of the Division of Nephrology mentioned above; healthy human kidney tissue was obtained from archived tumor nephrectomy specimens from the Institute of Pathology of the University Hospital of Zurich.

Reagents. A comprehensive list of reagents is given in the Supplemental Materials.

Anti-PLA2R1 titer determination. Anti-PLA2R1 antibodies were detected using the EUROIMMUN immunofluorescence test as part of the clinical assessment of the patients and either reported as titer (samples from Zurich and Bern) or as positive or negative (samples from Basel). For a quantitative analysis of antibody levels, we used the anti-PLA2R1 ELISA from EUROIMMUN according to the manufacturer's instructions.

Cell culture. Conditionally immortalized human podocyte cell lines were provided by Moin Saleem (University of Bristol, Bristol, United Kingdom) and cultured as previously described (51). Four cell lines (AB, ATC, K30, and LY) from different donors were initially cultured and tested for PLA2R1 expression. Because no cell line showed significant expression of PLA2R1 at the protein level, we used lentiviral overexpression (see below) and performed all further experiments with the cell line LY (52). HEK293 (gift from Lisa Buvall, University of Miami Miller School of Medicine, Miami, Florida, USA) and HUVEC cells (purchased from PromoCell, C-12203) were cultured in DMEM supplemented with 10% FBS and 1% penicillin/streptomycin.

Lentivirus-mediated PLA2R1 overexpression. The complete sequence of human PLA2R1 packaged in the pLPCX plasmid with an N-terminal FLAG tag was subcloned into the VVPW lentiviral expression vector (gift from Luca Gusella, Mount Sinai Hospital, New York City, New York, USA). HEK293 cells grown to 70%–80% confluence were transfected with VVPW, the packaging plasmid psPAX2 (Addgene, 12260), and the envelope plasmid pCMV-VSV-G (Addgene, 8454) at a ratio of 3:2:1 respectively, using FuGENE HD transfection reagent according to the manufacturer's instructions. Differentiated podocytes were infected with PLA2R1 lentivirus particles in the presence of 8 μg/mL polybrene for 16 hours, followed by a change of medium. Infected cells were used in the experiments 72 hours after lentiviral infection.

siRNA transfection. Gene-specific Flexitube GeneSolution siRNAs were used at 50–100 nM in the presence of HiPerFect transfection reagent per the manufacturer's instructions. The efficiency of the gene knockdown was evaluated by Western blot.

Cellular complement assay. Podocytes were seeded in 60 mm tissue culture dishes or in 6-well plates on glass coverslips (for immunofluorescence analysis) and differentiated at 37°C (the nonpermissive temperature) for 10 days to around 70% confluence. Cells were

then infected with PLA2R1-containing lentivirus or with an empty virus. Then, 48 hours after lentiviral infection, cells were washed 2 times with PBS and were serum-starved overnight. The next day, the cells were washed 2 times with PBS and 2.5% of patient or control serum or isolated IgG4 at the indicated concentration was added to the cells in incomplete RPMI1640 medium followed by incubation at 37°C for 30 minutes. The cells were then washed 2 times with PBS, and 5% of NHS as a complement source in incomplete medium was added, followed by a further incubation at 37°C for the indicated time periods. Cells were then washed 2 times with PBS and lysed with RIPA buffer supplemented with protease and phosphatase inhibitor cocktail or fixed in 4% formaldehyde for immunofluorescence. Cell lysate protein concentrations were estimated using the Pierce BCA protein assay solutions and were analyzed further on a 10% SDS-PAGE gel and by Western blot.

MTT cell-killing assay. Podocytes overexpressing PLA2R1 were seeded at 5000 cells/well in a 96-well tissue culture plate and treated with 2.5% serum from a pMN patient with anti-PLA2R1 antibody titer of 1:1000 (2138 RU/mL) for 30 minutes. Cells were washed 2 times with PBS, various concentrations (5%–20%) of NHS as a source of active complement were added, and the cells were incubated overnight at 37°C. The next day, the cells were washed 2 times with PBS and the cells were incubated for 4 hours at 37°C in the presence of 0.5 mg/mL MTT. The formazan crystals were dissolved with DMSO and the plate was read using a plate reader at 540 nm. Cycloheximide (30 μg/mL) plus TNF-α (25 ng/mL) were used as an apoptotic stimulus for the positive control.

Complement pathway analysis. Various versions of gelatin veronal buffer (GVB; 141 mM NaCl, 0.1% gelatin, 1.8 mM sodium barbital, 3.1 mM barbituric acid, and 10 mM EDTA, pH 7.3–7.4) were used to assess the complement pathway involved in mediating sublytic podocyte injury. GVB plus calcium and magnesium (GVB++; containing no EDTA, but 0.15 mM calcium chloride and 0.5 mM magnesium chloride) was used to allow for the activation of all 3 pathways, whereas GVB supplemented with magnesium and EGTA (containing 0.1 M magnesium and 0.1 M EGTA) was used to study the calcium-independent alternative pathway while inhibiting the calcium-dependent classical and lectin pathways. GVB plus EDTA was used to inhibit all complement activation pathways. Both patient serum and NHS as a complement source were diluted in the proper GVB buffer, and the sublytic complement assay was performed as described above. Where indicated, 10 μg/mL recombinant human MBL (Sino Biological) was added to the buffer containing NHS to facilitate activation of the lectin pathway.

IgG4 purification. A separation column was loaded with CaptureSelect IgG4 affinity matrix beads. The beads were equilibrated with 5 column volumes of PBS. Patient serum was loaded onto the column. Ten column volumes of PBS were used to wash the beads. The flow-through and all washing steps were collected into separate tubes for analysis. IgG4 was eluted with 5 column volumes of 0.1 M glycine pH 3.0 buffer. The eluted IgG4 fractions were neutralized with 0.1 volume 1 M Tris pH 8.0 buffer. The IgG4 fractions were pooled and concentrated using a Pierce protein concentrator with a 30K MWCO (Thermo Fisher Scientific, 88529). The concentrated IgG4 solution was filter sterilized using a 0.22 μm filter and stored at 4°C. All the collected fractions were analyzed by SDS-PAGE followed by either Coomassie brilliant blue staining or by

Western blot detection with anti-human IgG subclass–specific antibodies. The protein concentration of eluted IgG4 was determined using BCA protein assay.

IgG4 deglycosylation. Purified IgG4 from pMN patients was treated with 5 U PNGase F (Sigma-Aldrich) in GlycoBuffer 2 (New England BioLabs) according to the manufacturer's instructions. Antibody integrity after the deglycosylation process was confirmed by repeating the anti-PLA2R1 ELISA with the deglycosylated IgG4.

IgG glycosylation analysis. In a preliminary experiment, IgG4 was purified from 3 high-titer anti-PLA2R1–positive membranous nephropathy patients and from 3 healthy individuals as described above and analyzed for glycan chains associated with IgG4 at the Functional Genomic Center at the University of Zurich. The glycan quantification was done using mAbsolute kit from Asparia Glycomics per the manufacturer's instructions and by peptide mass fingerprinting MALDI.

For validation purposes in a larger cohort, glycopeptide analysis was performed using nano liquid chromatography mass spectrometry (nanoLC-MS) as described previously (53). Briefly, 1 μL of plasma from patients with membranous nephropathy, patients with other kidney diseases, or healthy individuals was used. The IgG was captured using 2 μL Protein A Sepharose fast flow beads (GE Healthcare) for each sample in a 96-well plate. The isolated IgGs were proteolytically digested using 500 ng trypsin treated with N-p-Tosyl-L-phenylalanine chloromethyl ketone (Sigma-Aldrich) in the presence of 40 μL 25 mM ammonium bicarbonate. The IgG-trypsin mixture was incubated at 37°C for 17 hours. Next, 200 nL of the digest from each sample was injected into an Ultimate 3000 RSLCnano system (Dionex/Thermo Fisher Scientific) coupled to a quadrupole-TOF-MS (Maxis Impact HD; Bruker Daltonics) as described (53). The data preprocessing comprising retention time alignment, m/z calibration, targeted glycopeptide integration, and data quality control was performed using LaCyTools, as described previously (53, 54). The resulting spectra were included in the analysis when the total spectral intensity was higher than 3 times the intensity of the blank measurements and the fraction of analytes above signal-to-noise ratio (S/N) was within the average ± 2 times standard deviation. The analytes were integrated for all samples based on accurate mass (± 10 ppm) and isotopic pattern matching (IPQ < 0.2). Lastly, the relative intensities of individual glycoforms were determined based on total area normalization per each IgG subclass. The derived traits were computed based on the specific glycosylation pattern of each IgG subclass as follows: IgG4 galactosylation = (1/2 * (G1F + G1FN + G1FS) + (G2F + G2FN + G2FS + G2FS2))/(G0F + G1F + G2F + G0FN + G1FN + G2FN + G1FS + G2FS + G2FS2). IgG4 bisection = (G0FN + G1FN + G2FN)/(G0F + G1F + G2F + G0FN + G1FN + G2FN + G1FS + G2FS + G2FS2). IgG4 sialylation = (1/2 * (G1FS + G2FS) + (G2FS2))/(G0F + G1F + G2F + G0FN + G1FN + G2FN + G1FS + G2FS + G2FS2). IgG4 sialylation per galactose = IgG4 sialylation/IgG4 galactosylation.

To determine the glycosylation pattern of PLA2R1-specific IgG4, antigen-specific IgG4 was isolated using the EUROIMMUN anti-PLA2R1 ELISA as described earlier (55). We pooled serum from 5 patients because of the low yield of antigen-specific IgG4 in a preliminary experiment using serum from 1 patient. Next, 400 μL of serum from each of 4 patients and 800 μL of plasma exchange plasma from 1 patient with high PLA2R1 antibody levels were used to isolate IgG4 as described above, yielding a total of 342 μg. The IgG4 was concentrated using a Pierce protein concentrator 30K MWCO, diluted 1:10

using the ELISA kit dilution buffer, and loaded to 8 wells of the ELISA plate. The plate was incubated for 1 hour at 37°C, the supernatant was removed, and the plate was washed 3 times with PBS followed by 2 washes with ammonium bicarbonate (25 mM). The PLA2R1-specific IgG4 was eluted with 100 mM formic acid, and then subjected to buffer exchange to PBS and glycopeptide analysis.

Isolation of anti-PLA2R1-specific IgG4 for far-Western blot analysis and complement-binding experiments. The extracellular portion of PLA2R1 comprising the cysteine-rich, fibronectin type II, and CTLD1-3 domains (CysR-CTLD3 protein) was cloned into the FLAG tag-CMV-14 expression vector (pCysR-CTLD3-FLAG) and transfected to HEK293 cells. After 48 hours, 800 ng/mL of the selection antibiotic G418 (Geneticin) was added in order to establish a stable cell line. To generate the recombinant protein, HEK293 cells grown in regular DMEM containing 100 ng/mL G418 were collected and lyzed using lysis buffer (50 mM Tris-HCl pH 7.4, 150 mM NaCl, 1 mM EDTA, and 1% Triton X-100) supplemented with protease inhibitor cocktail. The cell lysate was centrifuged for 15 minutes at $14,000g$ and filtered through a 0.45 μm filter. The cleared cell lysate was incubated with 1 mL anti-FLAG M2 affinity (Sigma-Aldrich) for 2 hours at 4°C to capture the CysR-CTLD3-FLAG fusion protein. The resin was collected by filtration in an empty column and was washed with 10 mL TBS 4 times. The CysR-CTLD3 protein was eluted in 6 fractions of 1 mL 0.1 M glycine HCl, pH 3.5 containing 1 M Tris, pH 8.0. A 20 μL aliquot of eluate was applied to SDS-PAGE gel and stained with Coomassie blue to evaluate the CysR-CTLD3 protein concentration by comparison to a protein standard of known concentration. The eluate containing CysR-CTLD3-FLAG was concentrated and the buffer exchanged to 100 mM MOPS in a Spin-X UF concentrator (Corning). A CysR-CTLD3-FLAG affinity column was prepared by incubating 100 μg purified CysR-CTLD3-FLAG in 100 mM MOPS with Affi-Gel 15 (Bio-Rad) for 4 hours at 4°C, followed by blocking of reactive sites with ethanolamine HCl for 1 hour. The column was washed and stored in PBS containing 0.02% sodium azide. Total IgG4 purified as described above was loaded to the CysR-CTLD3-FLAG affinity matrix, washed with PBS, and eluted with 100 mM glycine HCl, pH 2.4/150 mM NaCl. The buffer was exchanged to PBS in a Spin-X UF concentrator.

MBL-IgG4 ELISA. Unfractionated IgG from a patient with anti-PLA2R1-positive membranous nephropathy was coated onto a Thermo Fisher Scientific F8 MaxiSorp Immuno Clear ELISA plate for 16 hours in coating buffer (100 mM Na_2CO_3/NaHCO₃, pH 9.6). The plate was washed 3 times with TBS containing 0.05% Tween-20 (TBST), and residual binding sites were blocked by incubation with PBS containing 0.5% BSA. Recombinant human MBL (rh-MBL, gift of Kazue Takahashi) (56) was added (2 μg/mL, 50 μL per well) to some wells with or without mannose (100 or 500 mM). Another ELISA plate was coated with IgG4 isolated from 2 patients with anti-PLA2R1-positive membranous nephropathy and incubated with rh-MBL in the presence of TBST/Ca²⁺ (0.05% Tween-20, 10 mM $CaCl_2$) or buffer containing 1 mM EDTA. Binding of MBL was detected with mouse monoclonal anti-MBL antibody (1:1000, Abcam, ab23457) and donkey anti-mouse IgG-HRP antibody (1:2000, Jackson ImmunoResearch, 715-035-150). The reaction was developed with tetramethylbenzidine substrate (Thermo Fisher Scientific) and terminated with 3M H_2SO_4. The OD was read at 450 nm.

Complement C4 ELISA. Each well of a Thermo Fisher Scientific F8 MaxiSorp Immuno Clear ELISA plate was coated for 16 hours with 0.2 μg of purified IgG4 diluted in coating buffer (100 mM Na_2CO_3/NaHCO₃, pH 9.6). Plates were washed 3 times with TBS containing 0.05% TBST. Residual binding sites were blocked by incubation with PBS containing 0.5% BSA. Serum from a healthy subject containing a high concentration of MBL was added to each well as a source of MBL and MASPs at a concentration of 5% in 20 mM Tris, 1 M NaCl, 10 mM $CaCl_2$, 0.05% Tween-20 (vol/vol) and incubated at 4°C overnight. After each step, plates were washed with TBST/Ca²⁺ (0.05% Tween-20, 10 mM $CaCl_2$). Human C4 (Sigma-Aldrich; $E_{280}^{1\%}$ = 10.3) was diluted 1:2000 in TBST/Ca²⁺/Mg²⁺ and 1.6 μL was added to each well and incubated at 37°C for 30 minutes. Rabbit anti-C4b (Abcam, ab66791) diluted 1:1000 in TBST/Ca²⁺/0.5% BSA was added to each well and incubated for 2 hours at 37°C. Mouse IgG at 1 mg/mL in TBST/Ca²⁺ was included to block potential rheumatoid factor–like sites on IgG4. Each well was paired with an identical well lacking calcium and containing 1 mM EDTA. After washing, donkey anti-rabbit IgG-HRP (Jackson ImmunoResearch, 711-035-152) diluted 1:2000 in TBST was added for 2 hours at 37°C. The reaction was developed with TMB substrate (Thermo Fisher Scientific), terminated with 3 M H_2SO_4, and the OD was read at 450 nm. Wells lacking IgG4 were used to measure background activity. In addition, to control for potential variations in the amount of IgG4 bound in each well, the IgG4 content was measured with sheep anti-human IgG4 (The Binding Site, AU009). All assays were performed in triplicates. C4 activation was calculated as the amount of C4b bound in the presence of calcium corrected for IgG4 content (Units$_{Ca2+}$ − Units$_{EDTA}$)/Units$_{IgG4}$).

Far-Western blot. Far-Western blot analysis was performed on purified IgG4 from normal control subjects and PLA2R1-specific IgG4 from patients with anti-PLA2R1–positive pMN. The purified IgG4 was mixed with reducing or nonreducing SDS sample buffer, boiled, cooled, and run on several lanes of precast SDS-PAGE gels (4%–15%, Bio-Rad). The resolved protein bands were transferred onto nitrocellulose membranes (0.45 μm) and blocked with Carbo-Free blocking solution (Vector) for 1 hour. The indicated lanes were incubated with 1 μg/mL rh-MBL at 4°C overnight. After washing with TBST, the lanes were immunoblotted with mouse monoclonal anti-MBL antibody (1:1000, Abcam, ab23457) and detected with donkey anti-mouse IgG-HRP antibody (Jackson ImmunoResearch, 715-035-150) and developed using ECL (Bio-Rad). The other lanes were either incubated with anti-MBL antibody without prior incubation with MBL (control for anti-MBL antibody specificity) or with donkey anti-human IgG-HRP (Jackson ImmunoResearch, 709-035-149) (direct visualization of electrophoreses patient IgG4).

cAMP ELISA. cAMP determination was performed using Abcam cAMP direct immunoassay kit (ab65355) as described by the manufacturer's instructions. Briefly, differentiated podocytes were cultured in 60 mm tissue culture dishes. The cells were loaded with C3aR1 or C5aR1 antagonists SB290157 or W54011, respectively, at 1 mM for 1 hour. Then 2.5 % of pMN patient serum (451 RU/mL) was added and the cells were incubated for 30 minutes at 37°C, 5 % CO2. The cells were washed 2 times with PBS and 5% of NHS as a complement source in incomplete medium was added, followed by a further incubation at 37°C for 1 hour. Then, the cells were lysed directly in the dishes using 500 mL 0.1 M HCl and the cell lysates were centrifuged at $14,000g$ for 10 minutes. The supernatants were removed and assayed for protein concentration using the BCA method. All the samples had a protein concentration greater than 1 mg/mL. Next, 100 mL of each sample was assayed for cAMP levels and the ELISA plate was read at OD 540 nm.

Author contributions

Acknowledgments

Address correspondence: Andreas D. Kistler, Kantonsspital Frauenfeld, Pfaffenholzstrasse 4, 8501 Frauenfeld, Switzerland. Phone: 41.52.723.7643; Email: andreas.kistlerweber@uzh.ch.

Immunofluorescence of cells and tissues. Differentiated podocytes grown on coverslips were washed 2 times with PBS and fixed in 4% formaldehyde solution for 10 minutes. After 2 times washing with PBS, the cells were permeabilized with 0.1% Triton X-100 in PBS for 10 minutes followed by 2 washes with PBS. The cells were blocked with 1% BSA for 1 hour. The primary antibodies were diluted in 1% BSA solution, added to the cells, and incubated overnight at 4°C. The next day, the cells were washed 3 times with PBS and fluorescently labeled secondary antibodies were added for 1 hour at room temperature. The cells were washed 3 times with PBS and mounted on a microscope slide.

Human kidney biopsy sections were deparaffinized and rehydrated in xylene with several exchanges in ethanol. Antigen retrieval was performed with 10 mM citric acid, 0.05% Tween-20 buffer. The endogenous peroxidase was blocked in 3% hydrogen peroxide in methanol. The tissues were permeabilized with 0.4% Triton X-100 in PBS containing 1% goat serum. Nonspecific binding was blocked with 5% goat serum in PBS. The primary antibodies were prepared in 1% goat serum in PBS and incubated at 4°C overnight. Biotinylated antispecies secondary antibodies were added for 1 hour at room temperature, followed by 1-hour incubation at room temperature with FITC-labeled streptavidin.

Two trained observers independently analyzed the sections in blinded experiments. At least 6 glomeruli from each patient were scored for fluorescent intensity using a scale from 0 to 3. A P value less than 0.05 was considered significant using nonparametric ANOVA.

Microscopy. Fluorescence images were obtained using a Leica SP8 upright confocal microscope and LAS AF software at the Center for Microscopy and Image Analysis at the University of Zurich.

RT-PCR. Total RNA was isolated using RNeasy mini kit (Qiagen) and 3 μg were reverse-transcribed into complementary DNA using qScript SuperMix (Quantabio). The primers were designed using Oligo-Analyzer tool from Integrated DNA Technologies (IDT) and ordered from IDT. Primer sequences are given in Supplemental Table 1.

Statistics. Statistical analyses were performed using PRISM software (GraphPad) and SSPS version 25 (IBM). The data are expressed as mean ± SEM and analyzed using 1-way ANOVA followed by Tukey's post hoc analysis or Mann-Whitney U test as indicated. A P value less than 0.05 was considered significant.

Study approval. All patients gave written informed consent for biobanking of their sera and tissue. All studies were approved by the Kantonale Ethikkommission Zurich (approval number KEK-ZH-Nr. 2015-0385).

1. Couser WG. Primary membranous nephropathy. *Clin J Am Soc Nephrol*. 2017;12(6):983–997.
2. Ponticelli C, Glassock RJ. Glomerular diseases: membranous nephropathy—a modern view. *Clin J Am Soc Nephrol*. 2014;9(3):609–616.
3. Ronco P, Debiec H. Molecular pathogenesis of membranous nephropathy. *Annu Rev Pathol*. 2020;15:287–313.
4. Beck LH Jr, et al. M-type phospholipase A2 receptor as target antigen in idiopathic membranous nephropathy. *N Engl J Med*. 2009;361(1):11–21.
5. Beck LH Jr, Salant DJ. Membranous nephropathy: from models to man. *J Clin Invest*. 2014;124(6):2307–2314.
6. Borza DB. Alternative pathway dysregulation and the conundrum of complement activation by IgG4 immune complexes in membranous nephropathy. *Front Immunol*. 2016;7:157.
7. Meyer-Schwesinger C, et al. A novel mouse model of phospholipase A2 receptor 1-associated membranous nephropathy mimics podocyte injury in patients. *Kidney Int*. 2020;97(5):913–919.
8. Segawa Y, et al. IgG subclasses and complement pathway in segmental and global membranous nephropathy. *Pediatr Nephrol*. 2010;25(6):1091–1099.
9. Moseley HL, Whaley K. Control of complement activation in membranous and membranoproliferative glomerulonephritis. *Kidney Int*. 1980;17(4):535–544.
10. Jennette JC, Hipp CG. Immunohistopathologic evaluation of C1q in 800 renal biopsy specimens. *Am J Clin Pathol*. 1985;83(4):415–420.
11. Doi T, et al. Distribution of IgG subclasses in membranous nephropathy. *Clin Exp Immunol*. 1984;58(1):57–62.
12. Heja D, et al. Monospecific inhibitors show that both mannan-binding lectin-associated serine protease-1 (MASP-1) and –2 are essential for lectin pathway activation and reveal structural plasticity of MASP-2. *J Biol Chem*. 2012;287(24):20290–20300.
13. Ma H, et al. The role of complement in membranous nephropathy. *Semin Nephrol*. 2013;33(6):531–542.
14. Val-Bernal JF, et al. C4d immunohistochemical staining is a sensitive method to confirm immunoreactant deposition in formalin-fixed

paraffin-embedded tissue in membranous glomerulonephritis. *Histol Histopathol*. 2011;26(11):1391–1397.

15. Hayashi N, et al. Glomerular mannose-binding lectin deposition in intrinsic antigen-related membranous nephropathy. *Nephrol Dial Transplant*. 2018;33(5):832–840.

16. Lhotta K, et al. Glomerular deposition of mannose-binding lectin in human glomerulonephritis. *Nephrol Dial Transplant*. 1999;14(4):881–886.

17. Malhotra R, et al. Glycosylation changes of IgG associated with rheumatoid arthritis can activate complement via the mannose-binding protein. *Nat Med*. 1995;1(3):237–243.

18. Yu SM, et al. Proteinuric kidney diseases: a podocyte's slit diaphragm and cytoskeleton approach. *Front Med (Lausanne)*. 2018;5:221.

19. Saran AM, et al. Complement mediates nephrin redistribution and actin dissociation in experimental membranous nephropathy. *Kidney Int*. 2003;64(6):2072–2078.

20. Doublier S, et al. Nephrin redistribution on podocytes is a potential mechanism for proteinuria in patients with primary acquired nephrotic syndrome. *Am J Pathol*. 2001;158(5):1723–1731.

21. Cybulsky AV, et al. Experimental membranous nephropathy redux. *Am J Physiol Renal Physiol*. 2005;289(4):F660–F671.

22. Kistler AD, et al. Transient receptor potential channel 6 (TRPC6) protects podocytes during complement-mediated glomerular disease. *J Biol Chem*. 2013;288(51):36598–36609.

23. Pippin JW, et al. DNA damage is a novel response to sublytic complement C5b-9-induced injury in podocytes. *J Clin Invest*. 2003;111(6):877–885.

24. Cybulsky AV, et al. The actin cytoskeleton facilitates complement-mediated activation of cytosolic phospholipase A2. *Am J Physiol Renal Physiol*. 2004;286(3):F466–F476.

25. Quigg RJ, et al. Anti-Fx1A produces complement-dependent cytotoxicity of glomerular epithelial cells. *Kidney Int*. 1988;34(1):43–52.

26. Maverakis E, et al. Glycans in the immune system and the altered glycan theory of autoimmunity: a critical review. *J Autoimmun*. 2015;57:1–13.

27. Moller-Kristensen M, et al. On the site of C4 deposition upon complement activation via the mannan-binding lectin pathway or the classical pathway. *Scand J Immunol*. 2003;57(6):556–561.

28. Biermann MH, et al. Sweet but dangerous — the role of immunoglobulin G glycosylation in autoimmunity and inflammation. *Lupus*.

2016;25(8):934–942.

29. Faul C, et al. The actin cytoskeleton of kidney podocytes is a direct target of the antiproteinuric effect of cyclosporine A. *Nat Med*. 2008;14(9):931–938.

30. Sever S, et al. Proteolytic processing of dynamin by cytoplasmic cathepsin L is a mechanism for proteinuric kidney disease. *J Clin Invest*. 2007;117(8):2095–2104.

31. Li K, et al. Cyclic AMP plays a critical role in C3a-receptor-mediated regulation of dendritic cells in antigen uptake and T-cell stimulation. *Blood*. 2008;112(13):5084–5094.

32. Peng Q, et al. Dendritic cell function in allostimulation is modulated by C5aR signaling. *J Immunol*. 2009;183(10):6058–6068.

33. Yang Y, et al. IgG4 anti-phospholipase A2 receptor might activate lectin and alternative complement pathway meanwhile in idiopathic membranous nephropathy: an inspiration from a cross-sectional study. *Immunol Res*. 2016;64(4):919–930.

34. Bally S, et al. Phospholipase A2 receptor-related membranous nephropathy and mannan-binding lectin deficiency. *J Am Soc Nephrol*. 2016;27(12):3539–3544.

35. Gudelj I, et al. Immunoglobulin G glycosylation in aging and diseases. *Cell Immunol*. 2018;333:65–79.

36. Parekh R, et al. Age-related galactosylation of the N-linked oligosaccharides of human serum IgG. *J Exp Med*. 1988;167(5):1731–1736.

37. Morigi M, et al. C3a receptor blockade protects podocytes from injury in diabetic nephropathy. *JCI Insight*. 2020;5(5):e131849.

38. Moll S, et al. No complement receptor 1 stumps on podocytes in human glomerulopathies. *Kidney Int*. 2001;59(1):160–168.

39. Java A, et al. Role of complement receptor 1 (CR1; CD35) on epithelial cells: A model for understanding complement-mediated damage in the kidney. *Mol Immunol*. 2015;67(2 Pt B):584–595.

40. Takano T, et al. Complement-mediated cellular injury. *Semin Nephrol*. 2013;33(6):586–601.

41. Donoviel DB, et al. Proteinuria and perinatal lethality in mice lacking NEPH1, a novel protein with homology to NEPHRIN. *Mol Cell Biol*. 2001;21(14):4829–4836.

42. Asanuma K, et al. Synaptopodin regulates the actin-bundling activity of alpha-actinin in an isoform-specific manner. *J Clin Invest*. 2005;115(5):1188–1198.

43. Ning L, et al. Synaptopodin is dispensable for normal podocyte homeostasis but is protective in the context of acute podocyte injury. *J Am Soc Nephrol*. 2020;31(12):2815–2832.

44. Reiser J, Sever S. Podocyte biology and pathogenesis of kidney disease. *Annu Rev Med*. 2013;64:357–366.

45. Nakatsue T, et al. Nephrin and podocin dissociate at the onset of proteinuria in experimental membranous nephropathy. *Kidney Int*. 2005;67(6):2239–2253.

46. Cattran D, Brenchley P. Membranous nephropathy: thinking through the therapeutic options. *Nephrol Dial Transplant*. 2017;32(suppl_1):i22–i29.

47. Novak J, et al. Aberrant glycosylation of the IgA1 molecule in IgA nephropathy. *Semin Nephrol*. 2018;38(5):461–476.

48. Medjeral-Thomas NR, O'Shaughnessy MM. Complement in IgA nephropathy: the role of complement in the pathogenesis, diagnosis, and future management of IgA nephropathy. *Adv Chronic Kidney Dis*. 2020;27(2):111–119.

49. 2012 best practices for repositories collection, storage, retrieval, distribution of biological materials for research international society for biological environmental repositories. *Biopreserv Biobank*. 2012;10(2):79–161.

50. OECD guidelines on human biobanks genetic research databases. *Eur J Health Law*. 2010;17(2):191–204.

51. Saleem MA, et al. A conditionally immortalized human podocyte cell line demonstrating nephrin and podocin expression. *J Am Soc Nephrol*. 2002;13(3):630–638.

52. Haley KE, et al. Podocyte injury elicits loss and recovery of cellular forces. *Sci Adv*. 2018;4(6):eaap8030.

53. Falck D, et al. High-throughput analysis of IgG Fc glycopeptides by LC-MS. *Methods Mol Biol*. 2017;1503:31–47.

54. Jansen BC, et al. LaCyTools: a targeted liquid chromatography-mass spectrometry data processing package for relative quantitation of glycopeptides. *J Proteome Res*. 2016;15(7):2198–2210.

55. Scherer HU, et al. Immunoglobulin 1 (IgG1) Fc-glycosylation profiling of anti-citrullinated peptide antibodies from human serum. *Proteomics Clin Appl*. 2009;3(1):106–115.

56. Chang WC, et al. Lack of the pattern recognition molecule mannose-binding lectin increases susceptibility to influenza A virus infection. *BMC Immunol*. 2010;11:64.